Characterising the transcriptomic response of peripheral blood mononuclear cells to very low pH at single-cell resolution

Xiang (Shawn) Sun

Linacre College

University of Oxford

A thesis presented for the degree of

Master of Science by research

October 2024

This thesis is dedicated to my family, friends and colleagues who are supportive of my academic career all the way through.

Acknowledgements

In crafting this volume, which I believe would bridge a gap in immune response to acidity, I continue to profit from invaluable counsel of esteemed professionals. I am particularly grateful to Prof. Benjamin Fairfax for his continuous support of this single-cell experiment, as well as laborious criticism of the thesis. For sample preparation and cell culture, I owe a debt of gratitude to Dr. Surya Koturan, a former postdoctoral fellow in Fairfax group. Dr. Bo Sun and Dr. Esther Ng also deserve special recognition for selflessly sharing their bioinformatics scripts and for providing me with tips on how to improve the interpretability of my data analysis within a biological context. Additionally, thanks a lot to the Sygnature Discovery Team from Pathios Therapeutics for sample preparation protocols.

Surely, I would never have been able to complete this scientific venture without the loving support from all of my friends and colleagues in the Fairfax lab, including Akin-Adigun Oluwafemi, Dylan Muldoon, Guangyi Niu, Gusztav Milotay, James Gilchrist, Julia Bremke, Lea Cohen, Martin Little, Robert Watson, as well as Sophie Mackay. Great thanks to all of you!

Abstract

The tumour microenvironment (TME) is characterised by being acidic with pH as low as 6, which is accompanied by hypoxia, lactic acid accumulation and increased glycolysis levels. While previous studies have focused on the association between TME acidity and tumour development, our understanding of the transcriptomic response to environmental acidosis among immune cells is incomplete. Here, we have performed the first single-cell transcriptomic profiling of cultured peripheral blood mononuclear cells (PBMCs) in acidic environments, investigating molecular mechanisms underlying immune response to extracellular acidification. I have found that low pH is associated with distinct gene expression features, describing a conserved low pH-specific signature of 34 genes that was identified with differential expression (DE) analysis and high-dimensional weighted gene co-expression network analysis (hdWGCNA). Further, I described the cell types most transcriptomically affected by low pH, peforming UMAP visualization to identify pH-sensitive cell types, including normal and low pH-specific clusters. Subsequent transcription factor (TF) analysis using the package SCENIC, identified TF regulons in response to low pH, including *CREM* and *FOXO3*. Finally I explored the effect of single nucleotide variation at the gene *GPR65* that encodes a pH-sensitive G protein coupled receptor (GPCR) implicated in autoimmunity, describing genetically determined heterogeneity in acidity response. In summary, this project provides a novel transcriptomic reference to study the impact of acidity on transcriptomic response to low pH, which might be helpful for discovering novel targets associated with acidic TME.

Keywords — *tumour microenvironment, environmental acidity, low pH, single-cell RNA sequencing, peripheral blood mononuclear cells*

Table of Contents

List of Figures

1 | Introduction

1.1 Overview of acidic tumour microenvironment

The tumour microenvironment (TME) is a physical niche surrounding cancer cells, which includes a variety of non-cancerous immunosuppressive elements[1]. It consists of cancer-associated fibroblasts (CAFs), immune cells, blood vessels, lymphatic vessels as well as the extracellular matrix (ECM). All these TME components interact with each other to promote tumour growth and support immune evasion, forming a pro-tumour environment and protecting cancer from chemo-/radio- therapies[2]. Therefore, understanding the interplay between TME and tumour cells is important for cancer treatment, especially for tumour immunotherapy that includes immune checkpoint blockade (ICB), such as anti-CTLA4 and anti-PD1, and adoptive T cell transfer, like CAR-T treatment)[3]. It is difficult to overestimate the clinical impact of checkpoint immunotherapy, one of the greatest medical success with the 2018 Nobel Prize being awarded to James P. Allison and Tasuko Honjo in this field[4]. By boosting anti-tumour immune response in the TME, immunotherapy dramatically extends overall and progression-free survival time in multiple cancer types[5]. For example, the 5-year survival rate for metastatic melanoma has taken a huge leap, increasing from 5% in 2010 to 52% in 2019, which brings hope to patients with late-stage cancer[6,7]. Nonetheless, this therapeutic avenue is not successful for many patients. This is especially the case in cancers characterised by extensive local effects on non-tumour cells, which requires further investigation in the TME.

Cancer cells interact with various components in the TME, regulating multiple biological processes that help them grow, invade and evade host immune surveillance[8]. For instance, tumour cells secrete pro-angiogenic factors, such as the vascular

endothelial growth factor (VEGF), which stimulate the formation of new blood vessels[9,10]. Angiogenesis supplies tumour cells with essential oxygen and nutrients, promoting their growth; however, the newly formed blood vessels are always abnormal and leaky, resulting in heterogeneous TME regions of hypoxia and acidosis. Additionally, the TME also recruits a wealth of immunosuppressive cells to evade immune surveillance. Regulatory T cells (Tregs) are commonly activated in the TME with secretion of repressive factors, like TGF-β and IL-10, inhibiting the activity of effector T cells (especially CD8+ cytotoxic T cells) and weakening the anti-tumour immune response[11,12]. Myeloid-derived suppressor cells (MDSCs) might also expand in the TME, secreting inhibitory factors, such as inducible nitric oxide synthase (iNOS), reactive oxygen species (ROS) and arginase-1 (ARG1)[13]. Meanwhile, CAFs may change the ECM structure by secreting collagen and fibronectin, forming a physical barrier to prevent cytotoxic immune cells from entering the tumour core[14]. ECM remodelling also enhances the proliferation and invasion of tumour cells through stiffness-induced mechanosignalling[15]. Furthermore, tumour cells commonly upregulate immune checkpoint molecules in the TME, which bind to PD-1 or CTLA-4 on T cells, inhibit T cell activation, and dampen their anti-tumour response[16]. Also, tumour cells can evade the recognition of immune cells by downregulating major histocompatibility complex (MHC) molecules, making it difficult for the immune system to recognise them[17].

The TME feature we are studying in this project is environmental acidosis. Extracellular pH in normal tissues is well-regulated and maintained at a relatively constant range of 7.3 to 7.4[18]. In contrast, the TME is characteristic of being acidic with pH as low as 6[19]. Normal cells are mostly incompatible with extracellular acidosis, whereas tumour cells survive the acid-induced toxicity with uncontrolled proliferation and enhanced motility. In addition, tumour evasion of immune surveillance and reduced susceptibility to chemotherapy are also made

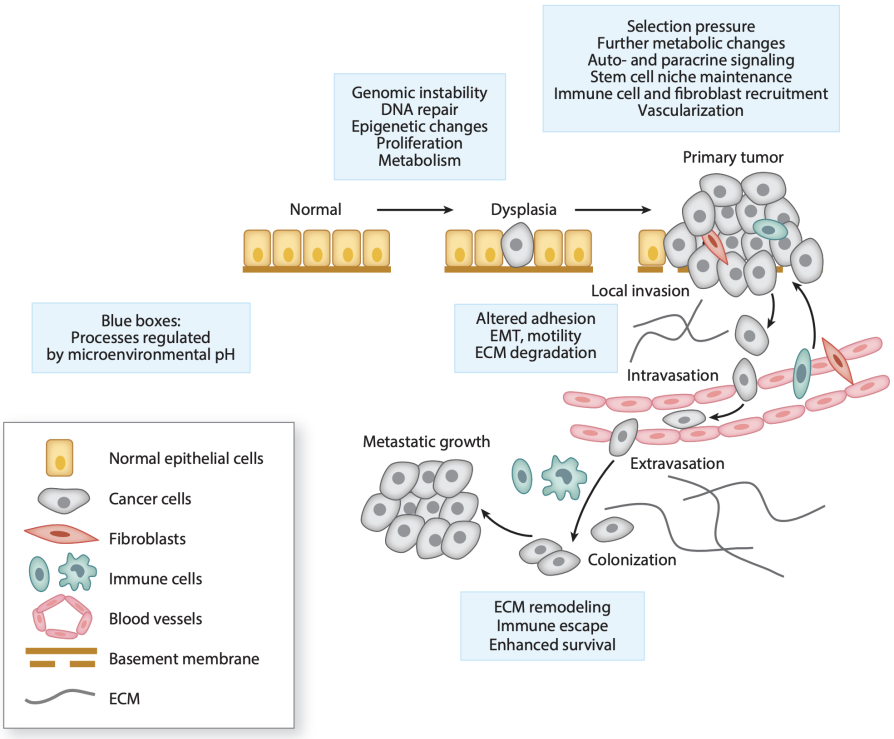

Figure 1.1: A simplified overview of TME acidosis-induced cancer progression. *It demonstrates how TME low pH leads to transition from preneoplastic lesions to metastatic tumours. Inside blue boxes are biological pathways in response to environmental acidification (Adapted from Boedtkjer and Pedersen[18]).*

possible by environmental low pH, as demonstrated by the decrease of cytotoxic effector cells and the partial suppression of anti-tumour cytokine secretion[20,21]. Furthermore, the manifestation of microenvironmental acidity is also accompanied by other signatures, such as hypoxia, fermentative glycolysis and increased lactate, which are all interconnected with each other[22,23]. Hypoxia, for instance, causes an increase in anaerobic glycolysis, which raises lactate levels and causes acidosis. Despite the widespread notion that hypoxic and acidic regions frequently coincide, certain acidic areas may also exist outside of hypoxic zones, suggesting a variety of formation mechanisms for microenvironments with partial low H^+ concentrations[24,25]. Besides, the production of CO_2 by aerobic glycolysis leads

to the build-up of H^+, particularly near the tumour-TME boundary where inadequate perfusion makes it difficult to eliminate oxidative metabolic wastes. As a result, blood flow and tumour metabolism alter spatiotemporarily along the course of cancer growth, making acidic TME components dynamic and heterogeneous[26].

In summary, the introduction section focuses on how environmental acidity promotes cancer cell development, and how low pH manipulates TME immune cells for immune escape (Figure 1.1). This might have implications for providing promising targets reversing acidic TME, enhancing anti-tumour treatment effects.

1.2 Molecular mechanisms of acidic TME

1.2.1 Formation of TME acidosis

Microenvironmental acidification is formed through a series of biochemical reactions (Figure 1.2). Tumour cells tend to switch their energy metabolism from aerobic respiration to glycolysis even with sufficient O_2, which is called the Warburg effect[27–29]. During glycolysis, glucose is broken down into lactate, which is an acidic metabolite[30]. Through lactate transporters, such as monocarboxylate transporters (MCTs), extracellular lactate accumulates and results in the TME acidification[31]. As the tumour grows, its centre area shifts away from the blood vessels, resulting in inadequate O_2 supply and the formation of hypoxic zones. Despite increased angiogenesis during cancer progression, the abnormal vessel structure leads to uneven distribution of oxygen and nutrients, rendering the tumour core in a state of hypoxia[32]. Insufficient O_2 supply activates hypoxia-inducible factor (HIF-1α) in tumour cells, which inhibits oxidative phosphorylation and further forces fermentative glycolysis[33,34]; meanwhile, under hypoxic conditions, tumour cells express high levels of carbonic anhydrase IX (CAIX) that catalyses the

reaction of CO_2 and water to produce carbonic acid (H_2CO_3), which can quickly dissociate into hydrogen ions (H^+) and bicarbonate (HCO_3^-), resulting in an increase in the acidity of the extracellular environment[35]. Moreover, in order to maintain homeostasis, tumour cells actively expel H^+ ions via proton pumps and transporters to prevent the intracellular pH from being too low. These proton pumps, like vacuolar ATPases and Na^+/H^+ exchangers, are often overexpressed in tumour cells, resulting in increased extracellular acidity[36–39].

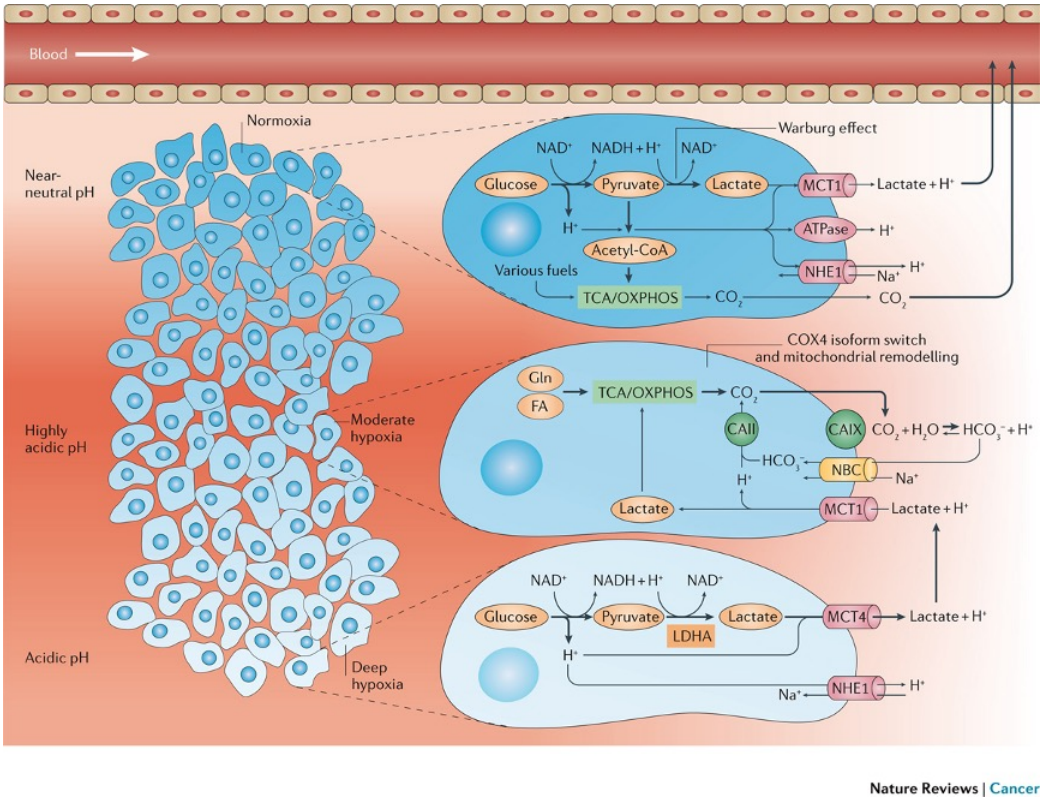

Figure 1.2: Biochemical reactions within an acidic TME. *This model depicts a biochemical model describing how TME acidification is formed through hypoxia, increased H^+ levels as well as lactate accumulation. Due to compositional heterogeneity within the TME, metabolite pathways are slightly different among near-neutral, acidic, and highly acidic regions (Adapted from Corbet and Feron[40]).*

1.2.2 Regulation of intra- and extra- cellular pH

Intracellular accumulation of lactate and CO_2 is detrimental to tumour cell survival, which requires export of acidic metabolic wastes. Through monocarboxylate transporters (MCTs) that are widely expressed on the tumour surface, lactate is transported to TME for relatively stabilizing intracellular pH[41]. Since CO_2 is non-polar, it diffuses through the lipid bilayer to external environment without consuming energy[42]; at the same time, tumour cells use Na^+/HCO_3^- cotransporters to absorb or excrete HCO_3^-, which helps to maintain the proper pH balance both inside and outside of the cell[43]. Moreover, as a subclass of the proton family, V-ATPases actively pump H^+ ions outside the tumour cell by hydrolysing ATP[38,39,44]. Another interesting fact is that tumoral intracellular pH is often higher than that of normal cells, as extreme TME acidification will lead to subsequent low pH inside tumour cells as well as restrictive proliferative function[43,45]. Thus, the intracellular pH of tumour cells is higher than that of normal cells in a TME zone of relatively neutral pH, while tumour cells in the low pH area will drop substantially with preserved metabolic abilities[18]. This phenomenon is particularly common when tumours spread from acidic primary sites to near-neutral organs.

1.3 The role of microenvironmental low pH in tumour development

1.3.1 Cancer genetics – from normal to dysplasia

The environmental acid-base status will cause genetic changes in pre-cancerous lesions, driving the transformation from normal epithelium to pre-neoplastic tissues. While gene mutations are frequently attributed to the early development of

tumours as well as the surrounding TME, the microenvironment itself also influences genetic alterations by increasing genomic instability, promoting oxidative stress and delaying DNA repair[46,47]. First, acidic conditions induce DNA double-stranded breaks (DSBs), a severe type of DNA damage that can easily lead to mutations and chromosomal aberrations. Previous studies have shown that activated topoisomerase II is involved in DNA breaks with exposure to low pH[48]. These aberrations can accumulate and promote malignant genetic changes during tumour progression. Secondly, the acidic microenvironment delays the repair process of DNA DSBs[49]. Especially in non-cancerous cells, the decrease in pH significantly delays the initiation of repair mechanisms, which may lead to the accumulation of DNA damage and gene mutations[37,50]. The acidic environment may interfere with the activity of DNA repair enzymes by affecting the intracellular pH, resulting in errors in the repair process[51]. Interestingly, environmental acidification will further inhibit the proliferation of normal cells that have not yet acquired oncogenic mutations; In contrast, tumour cells, which have already acquired mutations, can continue to proliferate under low pH, forming a selective advantage[52,53]. Thirdly, under acidic conditions, metabolic changes in cells can lead to an increase in ROS, which directly attacks DNA and causes oxidative damage[54]. If not repaired in time, these damages can be passed on to daughter cells through cell division, potentially promoting cancer evolution.

1.3.2 Cancer stem cell phenotype – from preneoplastic to primary tumour

Malignant cells are preferentially selected by evolutionary forces within the acidic TME, where cancer stem cells (CSC) play a pivotal role in driving primary tumour development[55]. The environmental acidification promotes metabolic reprogramming in cancer cells, which provides CSCs with survival advantage and therapy

resistance[56–58]. Hu et al.[56] discovered that the CYP24A1 (25-hydroxy vitamin D3-24-hydroxylase) - vitamin D pathway, which was activated by low pH, was crucial for preserving the cancer stemness with increased expression of markers, including *NESTIN, CD133* and *OCT4*. In stem-like glioma cells, CYP24A1 was increased during acidosis and facilitated the quick breakdown of $1\alpha,25(OH)_2D_3$, which was demonstrated to reduce the self-renewal ability, mitochondrial respiration and ATP generation. Consistent with the aforementioned result, TME acidification would also maintain glioma stem cell properties through heat-shock protein 90 (HSP90) activation[57]. A subsequent study showed that microenvironmental low pH caused melanoma cells to develop stem-like phenotype[59]. With a strong clonogenic and trans-differentiating potential both *in vivo* and *in vitro*, melanoma CSCs sustained by TME acidification overexpressed SOX2, which is essential for the maintenance of their oxidative metabolism. These findings indicate that extracellular low pH promotes stem cell-like properties in cancer, promoting primary tumour development.

1.3.3 Tumour invasion – from primary to metastatic tumour

TME acidosis plays a critical role in tumour invasion and dissemination from primary to metastatic tumours, colonizing other organs. Basically, extracellular low pH promotes the activity of matrix metalloproteinases (MMPs) and affects epithelial-mesenchymal transition (EMT). MMPs can degrade structural components of the ECM, which destroys the basement membrane and makes it easier for tumour cells to invade surrounding tissues[15,60]. Accordingly, acidic conditions are able to upregulate the expression and activity of MMPs, such as MMP-9, via phospholipase D-mitogen-activated protein kinase signaling[61]. In addition to ECM remodelling, environmental acidification also induces EMT by activating transforming growth factor-β (TGF-β)[62,63]. During the EMT process, tumour cells

change from the original adhesive epithelial phenotype to a mesenchymal property with a stronger migration ability, thereby enhancing their invasiveness[64]. These cells can pass through the ECM more easily and invade adjacent tissues. In fact, net H^+ outflow from tumour cells can create pH gradients that aid in directional migration from primary sites to metastatic colonies.

1.4 Immune Escape driven by TME acidification

1.4.1 Myeloid cells

While myeloid cells, such as macrophages and neutrophils, engulf foreign pathogens and cell debris under physiological circumstances, they undergo complex functional changes in acidic TME and are often hijacked by tumour cells for immune escape[65]. For example, acidosis-associated lactic acid, whether produced by mesenchymal stromal cells or tumour cells, have been demonstrated to drive functional polarization of tumour-associated macrophages (TAMs) into the pro-tumour M2-like phenotype[66,67]. During metabolic reprogramming and macrophage differentiation, expression of the hypoxia-related gene HIF-1α and pro-angiogenic gene *VEGF* is elevated in TAMs. In addition, myeloid-derived suppressor cells (MDSCs) are also involved in response to TME low pH. These activated MDSCs function more effectively with an increased level of iNOS, which further inhibits anti-tumour activity within the TME[68]. Congruent with this discovery, Husain et al.[69] have also found a significant reduction in MDSC cell counts with knock-down of lactate dehydrogenase A (LDHA) which produces extracellular lactic acid. It suggests extracellular accummulation of lactic acid and H^+ ions may increase the MDSC number for immune escape. To summarise, the pro-tumour effects of various myeloid cells in the TME can be greatly promoted by extracellular acidification.

1.4.2 Dendritic cells

In innate immunity, dendritic cells (DCs) are potent antigen-presenting cells that initiate adaptive immune response against tumours by sensing pathogen-associated molecular patterns (PAMPs) and damage-associated molecular patterns (DAMPs)[70]. But the specific mechanism of tumour-associated DCs is still unclear. While DC infiltration is positively associated with better survival outcomes for tumour patients, regulatory DCs in the TME also suppresses anti-tumour immune response by enhancing Treg activity[71–73]. There are several conflicting studies showing the effect of TME acidification on DC functions, which needs further investigation on different DC subsets[19,74]. It has been shown that treatment of lactic acid results in a DC immunosuppressive phenotype with reduced secretion of IL-12, which is similar to intra-tumoural DCs in multi-cellular tumour spheroids of melanoma and prostate cancer[75]. Likewise, Nasi et al.[76] have also found that DCs' endogenous production of lactic acid boosts the expression of IL-10 and hinders the capacity to migrate in response to CCL19. Nonetheless, opposite evidence has demonstrated that environmental acidification conversely elevates MHC-I-restricted antigen presentation in DCs, followed by anti-tumour T-cell activation[77]. In summary, low pH in the TME has an impact on DC's capacity to mature, differentiate and present antigens. Despite seemingly contradictory studies, tumour-associated DCs can be divided into various subtypes by single-cell sequencing and adopt various functional states in response to environmental acidity – it might be that some of these contradictory results reflect subset specific effects[78].

1.4.3 T cells

As a critical component of adaptive immunity, T cells recognize and destroy tumour cells with either direct killing by perforin/granzyme secretion or indirect ac-

tivation of immune response against cancer[79]. However, environmental acidosis tends to inhibit T cells through decreasing cytokine production and altering immune metabolism[5]. Fischer and colleagues[80] have discovered detrimental effects of microenvironmental lactic acid on human T cells with decreased expression of interleukin-2 (IL-2) and interferon-γ (IFN-γ). This aligns with a subsequent study where lactic acid produced by LDHA inhibits T-cell immune surveillance[21]. It has been proposed that LDHA-knockdown melanoma grows slower than control group via upregulation of IFN-γ as well as nuclear factor of activated T cells (NFAT). Moreover, as lactate exported by MCT-1 depends on the lactic acid concentration between T cell membranes, TME acidosis eliminates such electrochemical gradients, blocks lactate export and dampens ATP-producing glycolysis inside T cells[40,81]. Consistent with this argument, Ho et al.[82] have also reported that T cell exhaustion is associated with decreased levels of the glycolytic metabolite phosphoenolpyruvate (PEP). These studies, in total, summarize various molecular mechanisms of dysfunctional cytotoxic T lymphocytes (CTLs) in response to low pH within the TME.

1.4.4 Natural killer cells

Natural killer (NK) cells, which make up the first line of defence in the immune system, are special innate effector lymphocytes that combat tumours[83]. Under acidic conditions, tumour-infiltrating NK cell activity is inhibited by TME acidosis with sensitivity to extracellular acidic metabolites, such as lactic acid. Comparable to intra-tumoural cytotoxic T lymphocytes as mentioned above, environmental lactate reduces cytolytic activity of NK cells through decreasing expression of IFN-γ, granzymes and interferons[21,70]. In line with this study, Crane and colleagues[84] have also demonstrated that glioblastoma-secreted LDH5 generates lactic acid and inhibits natural killer group 2, member D (NKG2D) on NK cells.

This is significant for NK-mediated immune response against tumours. In contrast, short-term exposure to environmental acidification will enhance perforin degranulation in NK cells, which in turn improves killing of Cryptococcus neoformans and Cryptococcus gattii[85]. While such an acute increase in NK cell activity promotes host immune response against foreign pathogens during certain physiological processes (including wound healing), chronic exposure to TME acidification dampens the anti-tumour activity of NK cells[19].

1.4.5 B cells

Upon activation in normal tissues, B cells differentiate into plasma cells for antibody production, which neutralizes pathogens, activates the complement system, and clears abnormal cells[86]. But within the TME, B cells undergo complex functional and conformational alterations[87]. However, there is only limited indirect evidence on this topic. As demonstrated *in vitro* for the interaction between IgG and streptococcal protein G B1, environmental low pH significantly reduces its binding affinity via histidine-mediated electrostatic dissociation[88]. Thus, it seems plausible to speculate in a similar scenario that TME acidity may also lessen the therapeutic advantages of monoclonal antibodies (mAbs) against potential tumour targets. Also, considering physico-chemical properties of the acidic TME, it's also reasonable to hypothesize that environmental low pH creates an area of high fluid pressure and low O_2 supply, preventing mAb penetration into the tumour core[89]. These indirect studies and speculations suggest the anti-tumour activity of B cells and corresponding antibodies, as well as therapeutic monoclonal antibodies, might be inhibited by environmental low pH.

1.5 TME acidity and anti-tumour treatment

1.5.1 Chemotherapy and radiotherapy resistance

The acidic TME condition is closely associated with tumour's resistance to chemotherapies, which reduces their therapeutic effects through various molecular mechanisms. As for chemotherapy, an acidic environment would reduce medication absorption and increase drug efflux, which lowers the pharmaceutical concentration inside tumour cells and lessens its efficacy. To investigate the impact of the acidic TME on transport activity of daunorubicin, Thews et al.[90] exposed prostate carcinoma cells to pH 6.6 for 24h and observed a significantly increased transport rate, which in turn caused a drop in intracellular daunorubicin concentration. Meanwhile, the activity of P-glycoprotein (pGP), a crucial transporter member for daunorubicin, was remarkably raised through functional modulation. On the other hand, the acidic TME can also reduce the penetration of chemotherapy drugs into the tumour core by changing their physical and chemical properties[91]. When studying the factors that affect the entry of methotrexate into tumor tissues, it was discovered that an acidic environment inhibits the ATP-dependent active transport pathway, which lowers methotrexate absorption by tumour cells[92]. What's more, chemotherapy medications, such as doxorubicin, might be unstable in acidic TME, which reduces their pharmaceutical activity and reduces cytotoxic effects on tumour cells[93].

In addition to chemotherapy, sensitivity to radiotherapy is also affected by an acidic TME. Radiotherapy relies on free radicals (especially oxygen free radicals) to damage DNA and kill tumour cells. As O_2 is involved in the formation of free radicals, the generation of free radicals is reduced in an acidic and hypoxic region, where tumour cells become insensitive to radiotherapy[94]. In the meanwhile,

tumour cells under acidic conditions may repair DNA damage caused by radiotherapy by upregulating DNA repair pathways, such as ATM and ATR pathways, thereby improving tolerance to radiotherapy[95,96]. Moreover, acidic environments inhibit cell apoptosis and enhance tumour cell tolerance to gamma-irradiation by regulating apoptosis-related protein activity, such as p53 and caspase[97,98]. Exposed to experimental low pH, irradiated mouse breast cancer cells showed reversible inhibition of tumour cell apoptosis[99]. Consistent with the previous research, Park and colleagues[100,101] also found that extracellular pH 6.6 inhibited the release of human colorectal cancer cells from radiation-induced G2/M arrest more slowly than that of pH 7.5 via modifying the activity of cyclin B1-Cdc2 kinase. So, tumour apoptotic rates are slower when exposed to environmental acidosis. This suggests that the cell cycle arrest induced by the acidic environment may also be related to radiotherapy resistance.

1.5.2 Novel therapeutical methods targeting low pH

Despite anti-tumour treatment resistance caused by TME acidity, extracellular low pH can also be a promising target for novel therapeutics. In brief, there have been some indirect studies showing neutralization of microenvironmental low pH boosts immune checkpoint inhibitor (ICI) treatment. For instance, according to Pilon et al.[102], melanoma development in mice was inhibited by oral buffer treatment using 200 mmol/L sodium bicarbonate in drinking water. Furthermore, when combined with checkpoint inhibitors or adoptive T-cell transfer, bicarbonate monotherapy elevated microenvironmental pH and boosted T-cell infiltration in solid tumours, improving the rates of durable response to melanoma treatment[102,103]. Additionally, low extracellular pH might operate as a signal to anergize T cell functions by preventing the release of IFN-γ and TNF-α, and T cells could only be reactivated in an environment that is more alkaline[102,104]. When

mice were given systemic treatment with proton pump suppressors (H^+-ATPases inhibitors), TCR activation was made possible by elevated expression of IL-2Rα (CD25) and signal transducer and activator of transcription 5 (STAT5), which resulted in a considerable improvement in therapeutic effectiveness[104].

In addition to H^+ buffer therapy, the pH-sensitive drug delivery system also acts as an inspiring tool for precise medication administration. Take GALA as an example, a synthetic peptide with a glutamic acid-alanine-leucine-alanine repeat unit, which is engineered to interact with lipid bilayers at extracellular low pH in a preferential manner[105]. GALA-modified nanoparticles have been used in many fields of intracellular delivery, such as vaccines or small interfering RNA[106,107]. In addition, several acidosis-responsive polymer nanomaterials (examples of which include liposomes, polymer micelles) are also able to release encapsulated medications within a certain pH range[108]. Given that TME commonly has a lower pH than surrounding normal tissues, this can be helpful for the targeted delivery of drugs to tumours, boosting the efficacy of therapeutic drugs and reducing side effects on normal cells[109,110]. Liu et al.[111] designed Acetazolamide (ACE)-loaded pH-responsive nanoparticles (ACE-NPs), which quickly dissolves at pH 6.8 and releases ACE for inhibition of carbonic anhydrase IX. As a result, extracellular pH rises. Co-loaded with paclitaxel (PTX), ACE-NPs also result in better survival outcomes in mice in comparison to that of mice treated with PTX alone. These findings provide a new avenue for improving chemotherapy resistance in clinic.

Moreover, pH-related regulators (such as proton transporters) are also a potential target for reversal of TME acidity, which alleviates immunosuppression and assists in ICI treatment[112]. As revealed by single-cell RNA sequencing, SLC4A4 has been reported as the most highly expressed bicarbonate transporter in pancreatic ductal adenocarcinoma (PDAC), inhibition of which leads to TME acidity reversal[113]. On the one hand, the extracellular bicarbonate ions accumulate and

alkalinize TME by blocking the transport of bicarbonate ions from the extracellular space to the cytoplasm; on the other hand, the intracellular pH becomes acidic with decreased bicarbonate ions, which inhibits the production of lactic acid by LDHA-catalysed glycolysis, resulting in a decrease in extracellular lactic acid and a further reversal of the acidic microenvironment. To sum up, there is evidence to suggest that regulating pH-dependent transporters can modulate the acidic tumour microenvironment and enhance the anti-tumour effect of immunotherapy.

1.6 Aim and Objectives

Previous publications have already revealed the pivotal role of microenvironmental acidity across numerous aspects of cancer progression, from primary dysplasia to late-stage metastasis, through to reduced immunological response and acid-induced cell migration. However, most studies focus on the interplay between tumour cells and extracellular pH. Simplistic appraisal of immune response to low pH, especially in terms of transcriptome, has not been performed. There is still a lack of evidence in transcriptomic response to environmental acidosis among immune cells. Thus, in my MRes I have used single-cell RNA-seq to uncover potential mechanisms underlying pH-responsive immune features.

In brief, I would like to explore the following aspects:

- Are there any conserved transcriptomic features in response to low pH across all peripheral blood immune cells?
- Can I identify cell-type specific markers associated with environmental acidity in myeloid and lymphoid cells, respectively?
- How does environmental acidosis exert its immunosuppressive functions from the perspective of transcriptomics?

To tackle these questions, we have collected peripheral blood mononuclear cells (PBMCs) from 12 healthy donors and exposed them to extracellular acidity at pH 6.2; their transcriptomic and genetic profiles were assessed with single-cell sequencing and DNA array genotyping. With this single-cell dataset, I can compare transcriptomics between normal and low pH-exposed PBMCs, and investigate the effect of certain single nucleotide polymorphisms (SNPs) in low-pH response.

The analytical procedure (Figure 1.3) for this project is carried out as below: the single-cell dataset was first pre-processed from FASTQ files to a count matrix, followed by batch correction and cell type annotation. Differential expression was used to compare immune cells between normal and low pH. In addition to conventional enrichment analysis, we also performed gene regulatory network analysis for identifying pH-specific gene modules.

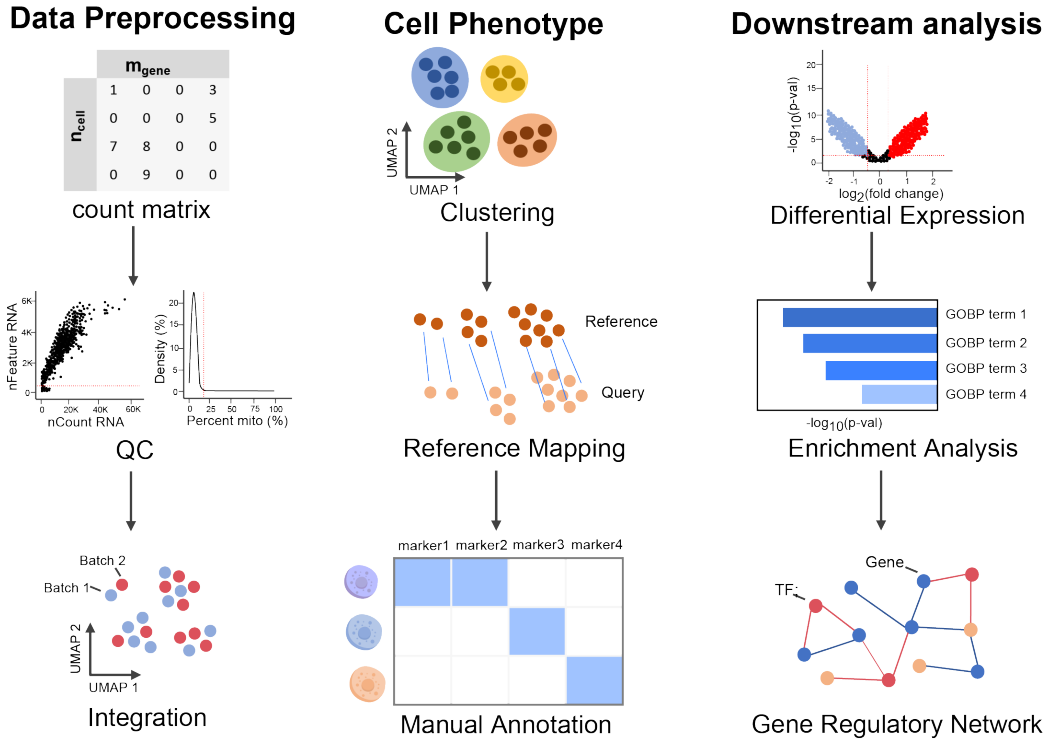

Figure 1.3: Schematic workflow of data analysis.

1.7 Thesis Outline

The remainder of this report is organised as follows:

Chapter 2 — introduces bioinformatics techniqeus and analysis strategies applied in this single-cell sequencing study.

Chapter 3 — describes immune subsets as well as cell subtypes, and defines pH-responsive clusters in both qualitative and quantitative manners at single-cell resolution.

Chapter 4 — identifies conserved and cell type-specific transcriptomic features in response to environmental acidification.

Chapter 5 — investigates the effect of the GPR65 SNP rs3742704 in transcriptomic response to extracellular low pH among immune cells.

Chapter 6 — discusses research limitations and potential future directions.

In brief, this report identifies significant gene modules and cell clusters that are associated with immune response to extracellular low pH, which might be applied as prospective tools for innovative cancer treatment approaches.

2 | Methods and Materials

2.1 Sample collection and preparation

This project was approved by the Research Committee of University of Oxford and Oxford Radcliffe Biobank (Research ethical approval number: 19/SC/0173 sub-project 19/A114). Peripheral blood samples were taken from 12 healthy donors with written consent for blood donation and data collection from Oxford Biobank (OCDEM). PBMCs were isolated by density gradient centrifugation using Ficoll at a speed 400g, 30min at RT and low acceleration and deceleration settings. The isolated PBMCs were then washed twice in cold HBSS buffer (300 g for 10 minutes at 4 °C) and used for cell culture. We prepared standard RPMI at pH 7.4 and in-house RPMI at acidic pH 6.2, adjusted with 10M HCl or NaOH, and buffered with HEPES or MES using the standardised protocol from our industry collaborators (Sygnature Discovery Team, Pathios Therapeutics). The PBMCs were cultured in RPMI-1640 medium with 10% FBS and 5% Penicillin-Streptomycin for 24h at 37 °C and 5% CO_2. Following the overnight culture, the cells were harvested and washed with HBSS to remove the traces of standard RPMI (at 300g, 10min at RT). The cells were then resuspended in medium with pH 6.2 or commercial RPMI at pH 7.4. This experiment was performed in time course at 4h and 24h. Cells were harvested and counted with Trypan blue staining using an automated cell counter to assess the viability prior to preparing the samples for single-cell suspensions. Using a 10x Chromium Single-cell 5' paired-end creation kit, single-cell transcriptome and VDJ libraries were created with 7 or 8 samples multiplexed per GEM, and sequenced at the Oxford Genomics Centre (Figure 2.1).

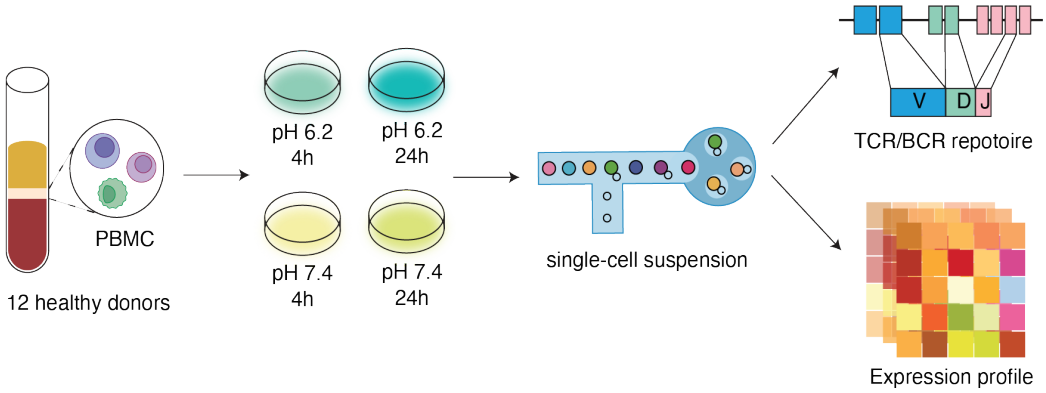

Figure 2.1: The experimental Workflow. *Cell culture conditions and the number of samples were denoted. Generally, PBMCs were collected from 12 healthy donors and cultured at low and normal pH for two time slots - 4h and 24h, respectively. Single-cell transcriptome and VDJ sequencing were performed for downstream data analysis.*

2.2 Single-cell RNA-seq data pre-processing

Single-cell RNA-seq data were aligned against the human genome GRCh38, followed by quantification using CellRanger (v7.1.0, 10x Genomics Inc)[114]. Cell barcodes were further recovered with the *EmptyDrops* function[115] in the DropletUtils package, including both CR- and ED-called cells. Next, accurate demultiplexing is essential to correctly assign each cell to its respective sample, thereby ensuring reliable downstream analysis. The cellsnp-lite program[116] was used for piling up bi-allelic SNPs on single cells, whilst donor deconvolution of pooled samples was carried out by vireo[117]. With vireo genotypic doublets as a gold standard, we next benchmarked different packages, including scDblFinder[118], scrublet[119] and DoubletFinder[120] for detection of heterotypic doublets. Comparing odds ratios between genotypic and heterotypic doublets, scDblFinder was chosen for identifying potential doublets in this single-cell dataset (Figure 2.2). To remove background noise, the SoupX package[121] was applied for ambient RNA correction.

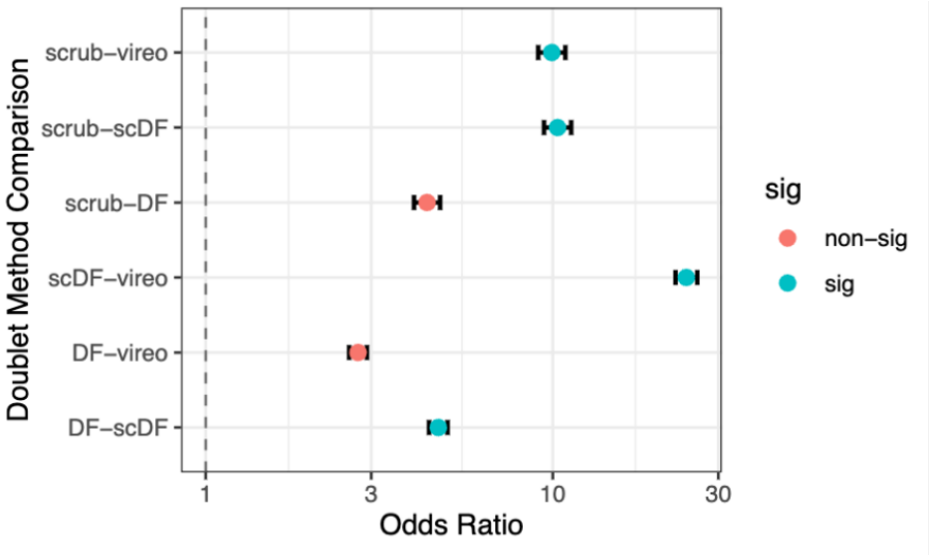

Figure 2.2: Odds ratio analysis of doublet detection. *Paired odds ratio (OR) analysis was performed between genotypic and heterotypic doublets. Single-cell data from pool 1 was taken as an example. scrub, srubelet; scDF, scDoubletFinder; DF, DoubletFinder.*

2.3 Unsupervised clustering and multi-sample integration

While the genes found in more than 5 cells were retained, two metrics were used to evaluate the quality of cells: 1) the proportion of mitochondrial gene counts less than 10%; 2) the number of identified genes larger than 300. Potential doublets were removed ahead of clustering, including heterotypic doublets identified by scDblFinder as well as genotypic doublets detected by vireo. Seurat v4.3.0[122] was then used for log normalization, scaling and determination of highly variable genes (HVGs) for dimensionality reduction. If not specified, 2,000 was the default value for HVG selection. To avoid potential confounding factors, variable features that match those in a pre-defined set of HLA/TCR/BCR-related genes were removed during downstream clustering. In addition, the effects of UMI counts,

mitochondrial gene ratios and cell cycle scores were also regressed out at the step of data scaling. Principal component analysis (PCA) was then applied on the HVG matrix to eliminate background noise, and the top 50 components were recruited for further analysis. Next, batch effects were corrected by the Harmony algorithm, designating each pool as the batch co-variate. Following application of Louvain clustering, cells were projected onto the UMAP space.

2.4 Cell cluster annotation

Cell clusters were characterized with both automatic and manual approaches: 1) supervised marker expression among populations; 2) unsupervised reference transfer with the integration-based Querymap function in Seurat. Given the overall gene expression similarity, query cells were matched to PBMC subsets identified in the Azimuth reference dataset[122], from which broad cluster identity was determined. Following reference mapping, we then manually annotated 6 primary cell types using canonical marker genes, including *CD3D, CD3E, CD3G, CD8A, CD8B* for T cells; *GNLY, NKG7, FGFBP2, KLRK1, PRF1* for NK cells; *LYZ, CD14, CLEC10A, THBS1, CSF1R* for myeloid cells; *MS4A1, CD79A, CD19, CD74, BANK1* for B cells; *HBB, HBA1, HBA2* for red blood cells (RBCs); *PPBP, PF4, TUBB1* for platelets; *GAB2, GATA2, RUNX1, IL3RA* for hematopoietic progenitor cells. Both RBCs and platelets in our single-cell dataset concurrently expressed T-cell markers, which might represent possible doublets, in line with earlier findings showing enhanced adhesion between RBC/platelets and T cells in a cultured environment.

I next extracted 4 major immune cell types, including T, B, myeloid as well as NK cells, and re-clustered them for further identification of cell subpopulations. Different clustering criteria were employed due to distinct numbers and charac-

teristics for each cell type. As a guide, we used publicly available PBMC scRNA-seq datasets, including COMBAT[123] and Azimuth[122]; resolutions were determined when canonical immune subtypes were recapitulated in our cohort. Notably, several clusters with expression patterns matching multiple cell types were treated as heterotypic doublets and removed from UMAP visualization, in spite of their potential function in immune perturbations[124]. For myeloid cell clustering, we recruited top 14 PCs (resolution = 0.3) at the first round of clustering, where we identified 2 clusters (Mono-T doublets) with concurrent expression of *LYZ, CD16, CD3D* and T-cell receptors; they were deleted from further analysis and followed by a second round of clustering (resolution = 0.1). For B cell clustering, top 14 PCs were selected (resolution = 0.1) at the initial round of clustering; an LYZ+ CD79A+ cluster (Mono-B doublets) was further expurgated for another round of clustering (resolution = 0.1). For NK cell clustering, we conducted Louvain clustering with top 10 PCs (resolution = 0.1). For T cell clustering, top 20 PCs were chosen at the first round of clustering (resolution = 1.5); we subsequently removed three clusters of T-Mono doublets and carried out an additional round of clustering (resolution = 0.9).

As a result, we identified 6 B, 3 NK, 11 CD4+ T, 6 CD8+ T, 2 MAIT, 1 gdT, 4 monocyte and 2 DC clusters. Next, the FindAllMarkers function in Seurat was utilized to identify cluster-specific differential expression (DE) genes. Cell subtypes were annotated using cluster-specific markers obtained from differential expression analysis on each cell cluster. To further cross-validate cell cluster annotation, enrichment over-representation analysis (ORA) was further conducted with MSigDB C8 cell type signature gene sets.

2.5 Enrichment of clusters across conditions

This protocol of odds ratio (OR) analysis was adapted from Zheng et al[125]. OR was computed to characterize group distribution of cell clusters, representing condition preference. A 2 by 2 table was created for every combination of cluster m and group n, which included the number of cluster m cells in group n, the number of cluster m cells in other groups, the number of non-m cluster cells in group n, and the number of non-m cluster cells in other groups. Following this, this contingency table was subjected to Fisher's exact test, producing OR along with its p-value. The R function p.adjust was utilized to apply the Benjamini-Hochberg (BH) approach for adjusting P-values. Here, we set the OR threshold to 2.5 with p.adj values < 0.05, which indicated that a cell cluster m with a significant OR > 2.5 was preferentially distributed in group n.

2.6 Gene module analysis

Gene modules specific to low pH were identified by high dimensional weighted gene co-expression network analysis (hdWGCNA)[126]. It was performed to construct a signed network at single-cell resolution for myeloid, T, B and NK cells, accordingly. All module eigengenes were corrected against individual samples with the Harmony algorithm, while top 25 genes were selected as hub genes in each module according to eigengene-based connectivity. The Spearman test was conducted to assess correlations between gene modules and low pH conditions. Each cell was given a module score based on top 25 hub genes by the function ModuleExprScore (method = "UCell").

2.7 Transcription factor regulon network

The SCENIC's python package[127] was used to perform regulon network analysis. With the raw single-cell count matrix as input, the grn command was used to calculate the gene-gene co-expression associations between transcription factors (TF) and their downstream putative targets. Following selection of TF-target pairings with a significance score (adjacent edges between TFs and genes) greater than 1, the ctx command defined regulons containing a single TF and downstream genes with RcsiTarget. The motif annotation database motifs-v10nr_clust-nr.hgnc-m0.001-o0.0.tbl and the ranking database hg38_10kbp_up_10kbp_down_full_tx_v10_clust.genes_vs_motifs.rankings.feather were used as a reference. Upon regulon identification, the active gene networks were determined as the average normalized expression of target genes by the aucell command. The regulon specificity scores (RSS) were further calculated using the R function calcRSS.

2.8 Differential gene expression analysis

For differential expression analysis in single-cell data, we applied a generalized linear mixed model $lmer(expr\ condition + (1|ID))$ with each donor used as a random variable with the whole dataset where indicated. In particular, the more cells we have, the more DEGs we obtain. Hence, in order to correct for count bias when comparing transcriptomic response across cell types, we also conducted cell subsampling with bootstrapping, where the single-cell count matrix was downsampled to the same number of cells across comparator groups over 50 iterations. DEGs were identified with p.adj values less than 0.001. Following identification of significant differential genes, enrichment analysis was carried out using the hypergeometric test by the XGR package. The BH method was performed for cor-

recting P-values. Significantly enriched signaling pathways within Gene Ontology Biological Processes (GOBP) and Molecular Signature Database (MsigDB) Hallmark Gene sets were identified when adjusted p-values were less than 0.05.

2.9 Genotyping

Genotyping was conducted on the Illumina Global Screening Array 24 version 3 (Illumina) and used for sample deconvolution of pooled single-cell data. Genotypes were aligned to hg37 and checked for call frequency > 0.9, SNP missingness < 3%, MAF > 1%, and Hardy–Weinberg equilibrium (HWE) P > 10-20 using GenomeStudio v2.0 and PLINK v1.9; samples with call rates < 97% were eliminated from further analysis. Following quality control, imputation was carried out using the Michigan Imputation Server with Haplotype Reference Consortium (HRC) version 1.1 Build hg19 as a reference panel. SNPs were further filtered for MAF > 4%, HWE P > 10-10 and r2 > 0.7 and lifted-over to hg38.

2.10 Statistical analysis

R (v4.3.0) and Python (v3.1.0) were used for statistical analysis of sequencing data, while clinical data were sorted by Microsoft Excel. For categorical variables, Fisher's exact test was used to compare groups. For continuous variables, Wilcoxon rank-sum tests and student's t-tests were employed. If not specified, a value of $P < 0.05$ was deemed statistically significant. For all data, *p<0.05, **p<0.01, ***p<0.001, and ****p<0.0001. Data visualization was conducted with ggplot2, UpsetR, pHeatmap, ComplexHeatmap, corr and LinkET. Images were created using Microsoft Powerpoint and Adobe Illustrator.

3 | A single-cell landscape of cultured PBMCs in acidic environments

3.1 pH-responsive PBMC transcriptome profile at single-cell resolution

To investigate the immune cell type-specific response to environmental low pH, we used the 10X Chromium platform to perform single-cell RNA-sequencing. Considering the difficulty to modify pH values within the TME *in vivo*, peripheral blood mononuclear cells (PBMCs) were selected from 12 healthy donors and exposed to pH 6.2 and pH 7.4, respectively. In addition, we also cultured PBMCs in 2 time slots - 4h and 24h – to identify potential long-lasting transcriptomic features in response to extracellular acidification. Following quality control and unsupervised clustering, 134,295 live cells were obtained with 31 cell clusters (Figure 3.1a). To our expectation, top-ranked differentially expressed genes specific to each subset aligned with known cell type markers, such as CD3D, CD3E, CD3G for T cells, GNLY, NKG7, FGFBP2 for NK cells, LYZ, CD14, CLEC10A for myeloid cells, MS4A1, CD79A, CD19 for B cells (Figure 3.1b-c). I annotated 7 main cell types with reasonable cell count ratios, but only extracted 4 main immune cells (T, myeloid, B and NK) for further investigation, abrogating platelets, red blood cells (RBCs) as well as progenitor-like haematopoietic cells. Notably, RBC and platelet cell clusters showed co-expression and T markers, which indicated potential doublets. This could be either physical adherence to T cells that formed doublets, or RBC/platelet – T cell conjugation that induced inflammation[128–130]. With less than 2K cells, it was hard to determine which scenario suited our single-cell data, so I removed them from downstream analysis.

In addition, 2 cell clusters with 798 cells in total did not conform to any major PBMC subtypes, with distinguished expression of CLC, GATA2, HDC, SOX4, CYTL1. All these markers had been demonstrated to regulate differentiation of haematopoietic progenitor cells (HPCs)[131], so I annotated them as progenitor-like haematopoietic cells. Whilst PBMCs are mainly composed of mature immune cells, a small proportion of HPCs or incompletely differentiated cells might also be released from bone marrow and circulate in peripheral blood. Hence, such an annotation was plausible.

To unbiasedly establish the pH-sensitive peripheral blood immunoprofile, I integrated single-cell data with the commonly used Harmony algorithm, removing potential batch effects and preserving true biological variance. Without integration, different techniques and/or varying sequencing depths might result in cells of the same kind behaving significantly different across batches, even if they have similar transcriptomic profile[132]. Cells of identical types might get dispersed in clustering, leading them to be wrongly classified as distinct cell clusters. Therefore, I used the Harmony package for multi-sample integration[133]. Here, cell embeddings in Harmony are iteratively adjusted for batch elimination following PCA dimensionality reduction. In each iteration, this integration approach makes transcriptomic positions of similar cellular phenotypes closer across samples. Previous benchmarking reviews on multi-sample integration have already ranked current packages for batch removal, and Harmony is among the top[132,134]. In our single-cell case, I also checked its integration ability by comparing cell count density between simple merging and Harmony integration (Figure 3.1d). I assumed that the expected proportions of each pool contributing to each cluster should converge to the ratio of pools in total. Accordingly, there were two peaks on the cell proportional density plot, which complied with Batch1:Batch2 of 2.5:1 in this case. In summary, I have described the establishment of a large-scale pH-responsive single-cell atlas.

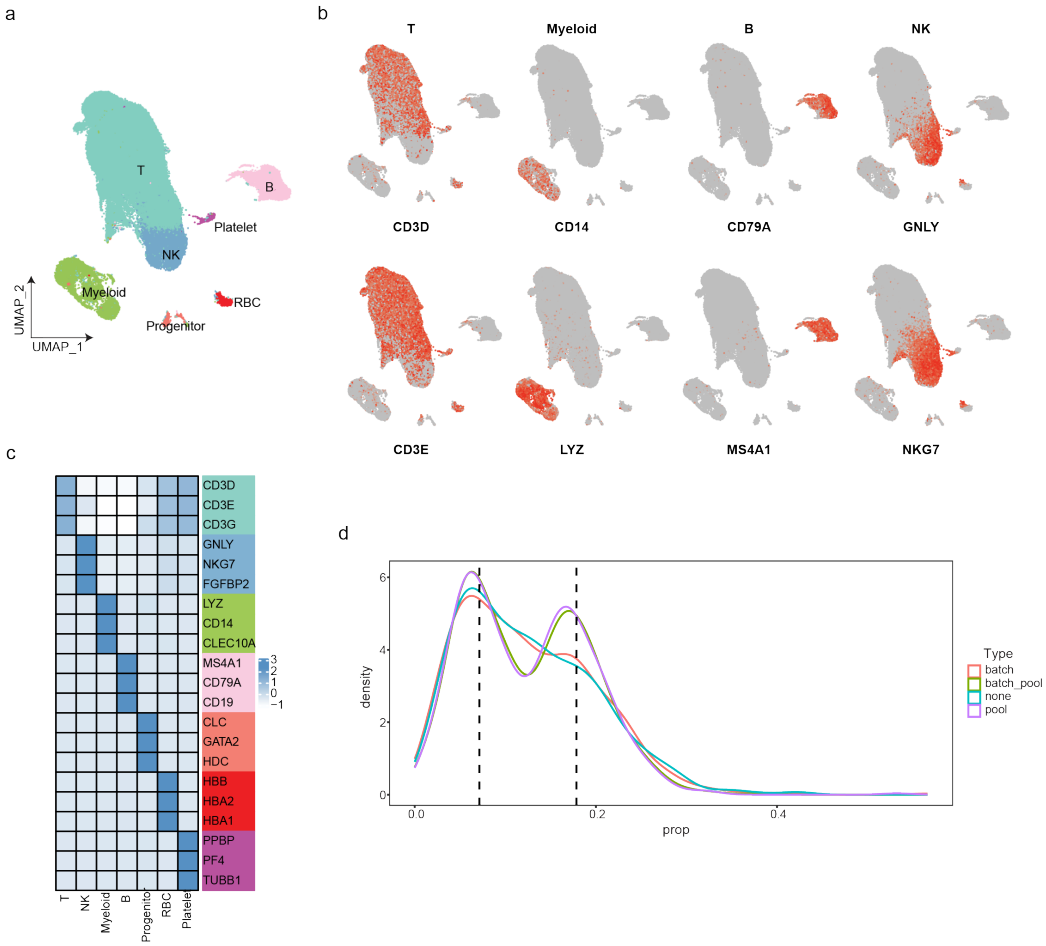

Figure 3.1: pH-responsive PBMC profile at single-cell resolution. ***a****, Uniform manifold approximation and projection (UMAP) plot showing main PBMC types, with each dot representing individual cells. NK, natural killer cells; RBC, red blood cells.* ***b****, UMAP visualization of canonical cell markers in each major cell population; normalized expression values were applied.* ***c****, Heatmap showing normalized expression of known cell markers in PBMC subsets.* ***d****, Density plot of cell proportions from each pool contributing to each cluster between Harmony integration and simple merging.*

There are few studies demonstrating the transcriptomic role of environmental acidosis in immune cells, and the transcriptome profile may provide novel insights into potential pH-sensitive immune targets within the TME.

3.2 Characterisation of immune cell subsets

Following extraction of 4 main immune subsets, I next performed a second round of clustering to identify re-fined cell subtypes induced by environmental acidosis (Figure 3.2a). Using the Azimuth[122] and Combat[123] datasets, clustering resolutions were established accordingly for each immune cell type, allowing us to replicate main immune subtypes in our own single-cell data. Given that these immune cells were cultured in acidic settings prior to single-cell sequencing, several cell clusters were uncharacterized by particular functional properties, especially in the context of T cells. Therefore, I first determined their immune meta type (such as naïve, effector and regulatory cells), and subsequently annotated them with cluster-specific markers upon DE analysis on each cell cluster, which reflected their potential biological characteristics induced by environmental acidosis. These genes could be either canonical cell type markers, like *CCR7* and *TRAV1-2*, or top-ranked cluster-specific DE genes, such as *CREM* and *THBS1*.

UMAP plots visualized distinct distribution of cell clusters between low and normal pH (Figure 3.2b). In myeloid cells, CD14+ monocytes were divided into low pH-specific (Mono_c01_CCL2) and normal pH-specific cell clusters (Mono_c03_CREM and Mono_c02_THBS1), while CD16+ monocytes as well as dendritic cells were evenly dispersed across pH ranges. For T cells, there was an upward trend of cell state transitions affecting both naïve and memory/effector-like T cells (including both CD4+ and CD8+ T cells); conversely, CD4_c11_FOXP3 Treg and $\gamma\delta$T gdT_c20_TRDV2 cell clusters seemed to be insensitive to extra-

cellular pH alterations. NK cells were simply split into $CD56^{bright}$ and $CD56^{dim}$ ones, and NK_c03_CREM appeared to be particularly sensitive to microenvironmental acidification. Within B cells, B_c02_ZEB1 was low pH-specific, whereas B_c01_KLF2 was mostly distributed in normal pH.

With qualitative identification of low and normal pH-specific cell clusters in UMAP plots, I subsequently applied odds ratio (OR) analysis for describing condition distribution preference in a quantitative manner (Figure 3.2c). I didn't just compare the number of cells in each group since cross-individual sequencing pooling led to imbalanced sample numbers as well as large within-group variance. Based on cell proportionate alterations, clusters with an OR value more than 2.5 were identified as pH-sensitive, whereas those with a threshold of less than 2.5 were resistant to environmental acidosis. With hierarchical clustering from perspectives of cell count alteration and gene expression profile, low and normal pH-specific were grouped together, respectively, which cross-validated the definition of pH-sensitive cell clusters. Accordingly, low pH-specific cell clusters seemed to exhibit immunosuppressive features comparable to those within the TME. For example, for CD8+ T naïve cells, cluster 12 progressed to cluster 13 with the marker *HMGB2*, which had been reported as a tumour prognostic marker, positively associated with tumour development and radioresistance[135–137]. Also, cluster 1 and 2 of CD4+ T naïve cells disappeared, whereas cluster 3 and 4 appeared, characteristic of histone-related genes and *CTSL*. This might contribute to stress response and metastatic invasion[138,139]. Intriguingly, the gene *CREM* seemed to be conserved among low pH-specific cell clusters, including Mono_c03_CREM, NK_c03_CREM, CD4T_c07_CREM, MAIT_c18_CREM. As a cAMP responsive element modulator, CREM encodes a TF that might regulate downstream gene expression within immunosuppressive environments[140]. So, I would further investigate CREM's impact on immune reactions to low pH in section 3.3.

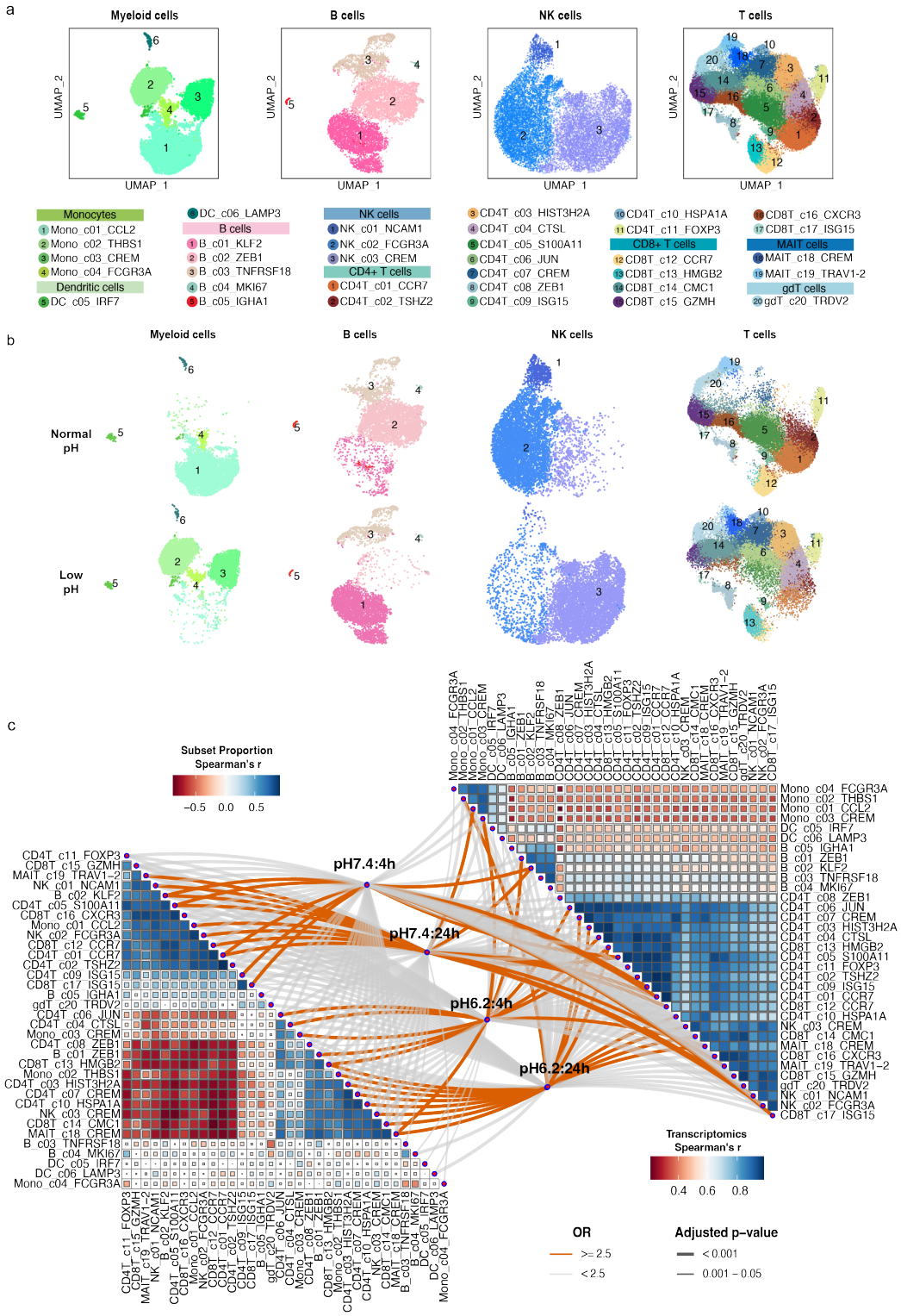
a
Myeloid cells
B cells
NK cells
T cells
UMAP_1
UMAP_2
Monocytes
1 Mono_c01_CCL2
2 Mono_c02_THBS1
3 Mono_c03_CREM
4 Mono_c04_FCGR3A
Dendritic cells
5 DC_c05_IRF7
6 DC_c06_LAMP3
B cells
1 B_c01_KLF2
2 B_c02_ZEB1
3 B_c03_TNFRSF18
4 B_c04_MKI67
5 B_c05_IGHA1
NK cells
1 NK_c01_NCAM1
2 NK_c02_FCGR3A
3 NK_c03_CREM
CD4+ T cells
1 CD4T_c01_CCR7
2 CD4T_c02_TSHZ2
3 CD4T_c03_HIST3H2A
4 CD4T_c04_CTSL
5 CD4T_c05_S100A11
6 CD4T_c06_JUN
7 CD4T_c07_CREM
8 CD4T_c08_ZEB1
9 CD4T_c09_ISG15
10 CD4T_c10_HSPA1A
11 CD4T_c11_FOXP3
CD8+ T cells
12 CD8T_c12_CCR7
13 CD8T_c13_HMGB2
14 CD8T_c14_CMC1
15 CD8T_c15_GZMH
16 CD8T_c16_CXCR3
17 CD8T_c17_ISG15
MAIT cells
18 MAIT_c18_CREM
19 MAIT_c19_TRAV1-2
gdT cells
20 gdT_c20_TRDV2
b
Normal pH
Low pH
c
Subset Proportion Spearman's r
−0.5 0.0 0.5
pH7.4:4h
pH7.4:24h
pH6.2:4h
pH6.2:24h
Transcriptomics Spearman's r
0.4 0.6 0.8
OR
>= 2.5
< 2.5
Adjusted p−value
< 0.001
0.001 − 0.05

Figure 3.2: Characterisation of immune cell subsets. ***a****, UMAP visualization of immune subset re-clustering. Cell clusters were annotated with canonical markers or top-ranked DE genes.* ***b****, UMAP plots split by pH conditions.* ***c****, Sandwich heatmap showing Spearman correlation among cell clusters from perspectives of cell counts and transcriptomics.*

3.3 Transcription factor regulons in low pH-specific clusters

After identifying specific immune subtypes enriched in both low and normal pH groups, an additional challenge is determining gene regulatory mechanisms underlying cell state alterations in response to environmental acidification. Thus, I used the python module of SCENIC[127] to infer the TF-based regulation network in 3 steps: 1) constructs a co-expression network between own single-cell data and known TFs; 2) uses RcisTarget to identify regulons that include a TF and downstream genes with upstream TF-binding sites; 3) measures the activity of TF regulons for each cell via AUCell scoring. To investigate the specificity of TF regulon activity in a particular cell population, I calculated the regulon specificity score (RSS) for each pH-sensitive cluster, and ranked them in a numeric order (Figure 3.3a). Interestingly, several regulons, such as CREM(+), FOXO3(+), FOSB(+), FOXA1(+) and HIF1A(+), frequently appeared among top-ranked TFs that were specific to low-pH clusters. This might indicate that these regulons are crucial regulators responding to low pH, rather than simply sustaining cell development or differentiation. Notably, the plus or minus signs in brackets represent TF-mediated upregulation or downregulation of downstream gene expression.

Furthermore, I visualized AUCell scores of interesting TFs on each pH-sensitive cell cluster (Figure 3.3b). Split by pH conditions, numerous regulons like CREM(+), FOXO3(+) and FOSB(+) seemed to be distinct between low and normal pH-

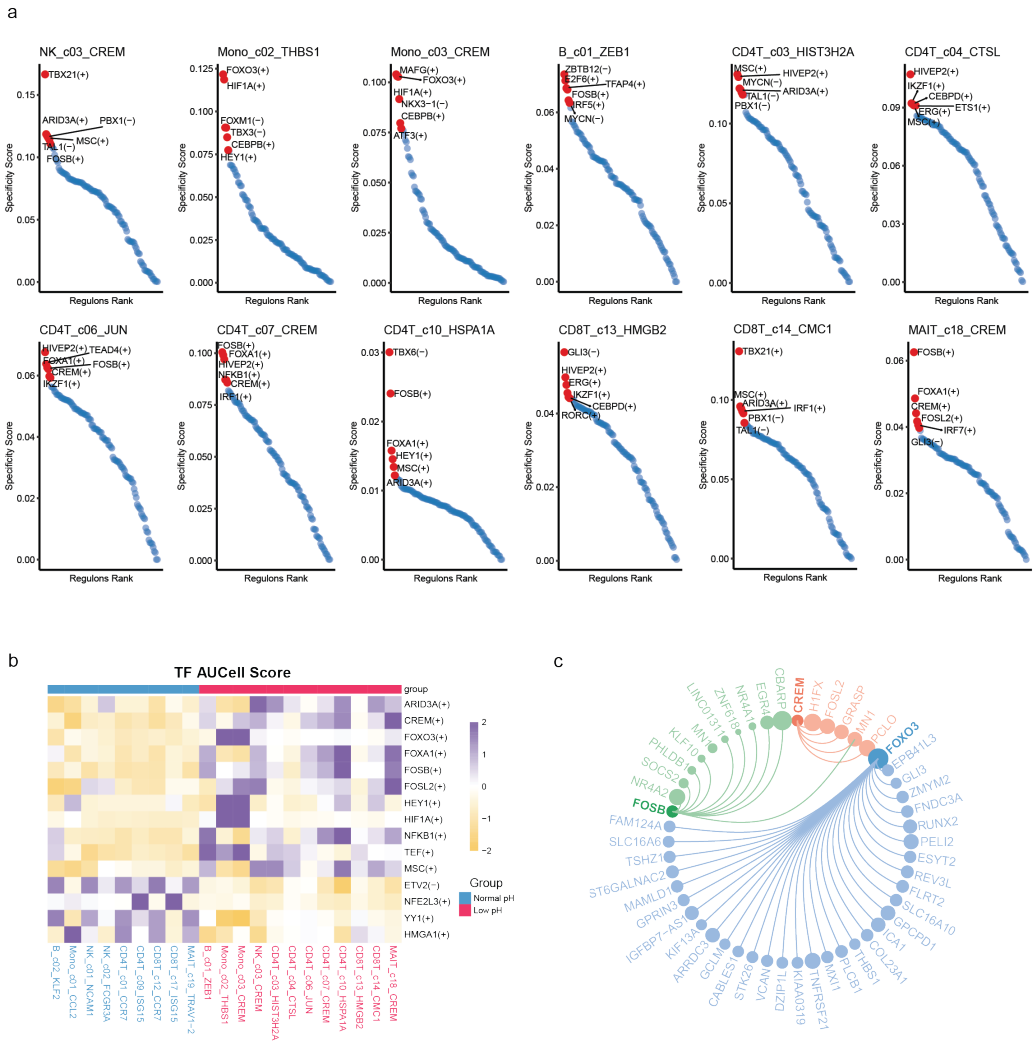

Figure 3.3: Transcription factor regulons in low pH-specific clusters. *a, Scatter plots of regulon specificity scores (RSS) for pH-sensitive cell clusters. Top 6 tanked TF regulons were highlighted. b, Heatmap showing AUCell scores of selected TF regulons in low pH-specific clusters. c, Circle plot demonstrating the gene regulatory network between TFs (including CREM, FOXO3 and FOSB) and downstream target genes in this single-cell cohort.*

specific clusters, and I further visualized their regulatory network in this single-cell dataset (Figure 3.3c). These TF regulons had been reported to induce cellular adaptation to acidic environments, cause immunosuppressive phenotypes and regulate apoptosis, all of which were comparable to features within the TME. For instance, Yu et al.[140] identified association between CREM and CD8+ T cell exhaustion that led to poor prognosis in gastric adenocarcinoma. It was also shown that FOXO3-induced FOXP3 activation would promote development of Treg and myeloid-derived suppressor cells (such as tumour-associated dendritic cells)[141–143]. What's more, mediated by TCR/CD3, FOSB with dimerization with c-Jun was also involved in activation-induced cell death that regulates lifespan of human T cells[144]. In summary, these discoveries all demonstrated that TF-regulatory signatures within the TME could be replicated in acidity-induced immune cells.

4 | Transcriptomic signatures in response to low pH

4.1 TME-like features induced by acidic environments

To identify genes and pathways upregulated in response to environmental acidification, I performed differential expression (DE) analysis in T, B, NK and myeloid cells, respectively. Beforehand I was studying cell clusters that were specific to low-pH response, now I took a step back looking at bulk myeloid and lymphoid cells. Notably, one major challenge here is the difficulty of deciding which approach to use for single-cell DE analysis – single-cell statistical tests, pseudo-bulk analysis or linear mixed models. Currently, there are some conflicting studies benchmarking various DE techniques in single-cell datasets, but no consensus has been reached on the best performing method. While Squair et al.[145] prioritized psudo-bulk analysis with bulk RNA-seq data as 'gold standard', the linear mixed model was also recommended to avoid pseudo-replicates derived from single-cell wilcox tests[146]. However, these two results are not completely contradictory, with each approach having its own pros and cons. On the one hand, generalized linear mixed models usually consume lots of computational resources and time; on the other hand, pseudo-bulk might be underpowered due to imbalance between individual samples with widely disparate cell populations. In summary, we could make decisions dependent on real circumstances of our own single-cell data.

Considering imbalanced individual cell counts in our single-cell data, I chose the linear mixed model $lmer(expr\ timepoint + (1|ID))$ here, as it was well-powered and avoided false discoveries during DE analysis. Generally, DE genes in 4h and 24h groups were overlapped to obtain long-lasting transcriptomic features, which

we paid close attention to. We visualized top6 ranked DE genes that were upregulated in both groups for each immune type (Figure 4.1a). Interestingly, expression of SLC16A family genes encoding monocarboxylate transporters were elevated in response to low pH among all immune cells, with lymphoid cells expressing more *SLC16A14* and myeloid cells expressing more *SLC16A10*. SLC16A-encoding monocarboxylate transporters would be predicted to facilitate transport of small molecules, such as lactate and pyruvate, upregulation of which suggested potential immune adaption to environmental acidification, especially in the context of tumour microenvironment or tissue inflammation[147]. In addition, histone-related genes, like *HIST1H2BM*, were frequently upregulated in the low-pH condition, which indicated transcriptional alteration in rsponse to acidity. Moreover, some other cell type-specific DE genes were also interesting in response to low pH. For example, upregulated *HES7* (hairy and enhancer of split 7) in T cells, which acted as a suppressor of the Notch signalling pathway in developmental biology, might also inhibit T-cell development in acidic TME[148]. Besides, I also found that *THBS1* (Thrombospondin 1) was highly expressed in low pH-cultured myeloid cells, which was comparable to myeloid-derived suppressor cells. As a multi-functional ECM protein, it is crucial in cell adhesion, apoptosis and immune escape within the TME[149]. By activating TGF-β activity, THBS1 could increase tumour-infiltrating monocyte-like cells, inhibiting anti-tumour immune response[150,151]. These results demonstrated a range of immunosuppressive characteristics brought on by microenvironmental acidity.

Upon differential expression analysis between low and normal pH groups, we still observed thousands of upregulated or downregulated genes for each cell. DE analysis is very sensitive and capable of detecting all genes with significant expression changes in response to acidosis[152]. However, not all up- or down-regulated genes

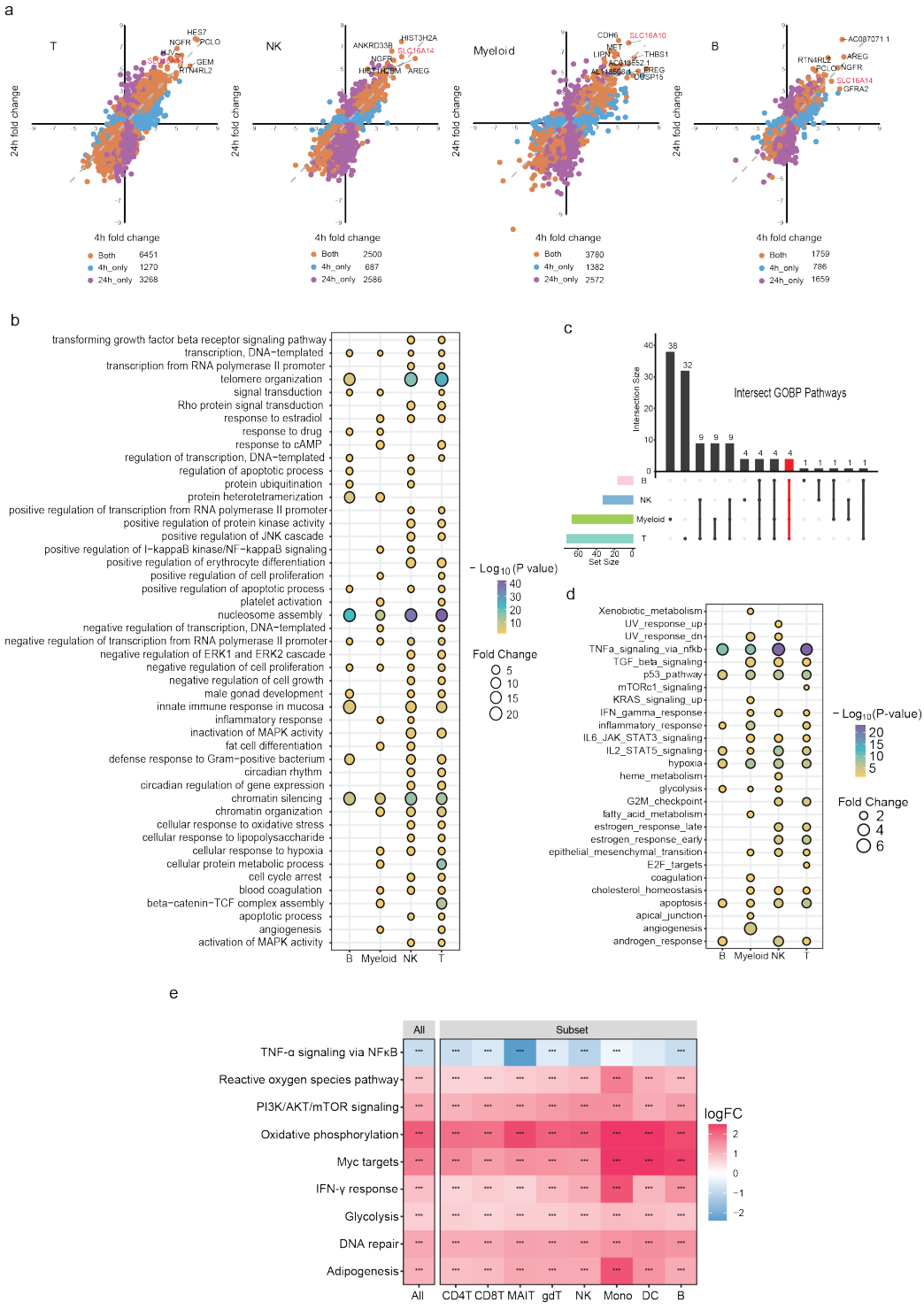
a
T
NK
Myeloid
B
24h fold change
4h fold change
Both 6451
4h_only 1270
24h_only 3268
Both 2500
4h_only 687
24h_only 2586
Both 3780
4h_only 1382
24h_only 2572
Both 1759
4h_only 786
24h_only 1659
b
transforming growth factor beta receptor signaling pathway
transcription, DNA−templated
transcription from RNA polymerase II promoter
telomere organization
signal transduction
Rho protein signal transduction
response to estradiol
response to drug
response to cAMP
regulation of transcription, DNA−templated
regulation of apoptotic process
protein ubiquitination
protein heterotetramerization
positive regulation of transcription from RNA polymerase II promoter
positive regulation of protein kinase activity
positive regulation of JNK cascade
positive regulation of I−kappaB kinase/NF−kappaB signaling
positive regulation of erythrocyte differentiation
positive regulation of cell proliferation
positive regulation of apoptotic process
platelet activation
nucleosome assembly
negative regulation of transcription, DNA−templated
negative regulation of transcription from RNA polymerase II promoter
negative regulation of ERK1 and ERK2 cascade
negative regulation of cell proliferation
negative regulation of cell growth
male gonad development
innate immune response in mucosa
inflammatory response
inactivation of MAPK activity
fat cell differentiation
defense response to Gram−positive bacterium
circadian rhythm
circadian regulation of gene expression
chromatin silencing
chromatin organization
cellular response to oxidative stress
cellular response to lipopolysaccharide
cellular response to hypoxia
cellular protein metabolic process
cell cycle arrest
blood coagulation
beta−catenin−TCF complex assembly
apoptotic process
angiogenesis
activation of MAPK activity
B Myeloid NK T
− Log10 (P value)
Fold Change
c
Intersect GOBP Pathways
Intersection Size
Set Size
d
Xenobiotic_metabolism
UV_response_up
UV_response_dn
TNFa_signaling_via_nfkb
TGF_beta_signaling
p53_pathway
mTORc1_signaling
KRAS_signaling_up
IFN_gamma_response
inflammatory_response
IL6_JAK_STAT3_signaling
IL2_STAT5_signaling
hypoxia
heme_metabolism
glycolysis
G2M_checkpoint
fatty_acid_metabolism
estrogen_response_late
estrogen_response_early
epithelial_mesenchymal_transition
E2F_targets
coagulation
cholesterol_homeostasis
apoptosis
apical_junction
angiogenesis
androgen_response
B Myeloid NK T
− Log10(P-value)
Fold Change
e
All
Subset
TNF-α signaling via NFκB
Reactive oxygen species pathway
PI3K/AKT/mTOR signaling
Oxidative phosphorylation
Myc targets
IFN-γ response
Glycolysis
DNA repair
Adipogenesis
All CD4T CD8T MAIT gdT NK Mono DC B
logFC

Figure 4.1: TME-like features induced by acidic environments. *a, Scatter diagram demonstrating log2 fold changes of significant DE genes when comparing between pH6.2 and pH7.4. Orange dots represent overlapped genes between both 4h and 24h groups, while 4h-only and 24h-only genes were shown by blue and purple dots, respectively. b, Dot plot of GOBP pathway enrichment for overlapped DE genes that were significantly upregulated in response to acidity. c, Upset plot of enriched GOBP pathways that were overlapped among immune subsets, with the red bar indicating 4 conserved biological processes involved in low-pH response. d, Dot plot of MsigDB Hallmark enrichment for overlapped significantly upregulated genes. e, Heatmap showing log2 fold changes for sores of selected TME-like signatures. Genes from MsigDB Hallmark gene sets were used to calculate the per-feature score for both pH6.2 and pH7.4 groups in each immune subset, and limma was applied for DE analysis. ***p<0.001.*

- which may incorporate a lot of background noise and genes with small effect sizes or lowly expressed - have true biological importance. Only a proportion of DE genes are directly associated with exposure to low pH. Thus, in section 4.3 and 4.4, I would also apply various methods of gene regulatory network, narrowing the scope of conserved or cell type-specific genes that are sensitive to low pH.

With long-lasting DE genes in response to low pH, I next conducted enrichment ORA to determine whether certain functional pathways are significantly enriched in upregulated genes. In the GOBP database, four conserved biological pathways were identified across immune cells, including chromatin silencing, negative regulation of cell proliferation, negative regulation of transcription from RNA polymerase II promoter, and nucleosome assembly (Figure 4.1b-c). It indicated potential alterations of the gene expression pattern in immune cells, which might inhibit cell proliferation and promote escape of immune surveillance. Also, there were other known acidosis-induced biological processes present in upregulated pathways, such as angiogenesis, apoptotic process, cellular response to oxidative stress and cell cycle arrest. All these enriched GOBP terms suggested that immune cells exposed to low pH would induce metabolic reprogrammed states proximal to those within the TME. Besides, with MsigDB Hallmark gene sets, I applied en-

richment analysis again to cross-validate GOBP results (Figure 4.1d). Similarly, hallmarks of cancer were activated in response to extracellular acidification, including hypoxia, apoptosis-related p53 pathway and glycolysis, all of which were conserved among immune cells. Additionally, angiogenesis seemed to be myeloid cell-specific; this was congruent with a previous study showing that myeloid cells secreted pro-angiogenic cytokines (such as VEGF, IL-6) to promote chronic inflammation and tumour development[153]. Another intriguing phenomenon was the discovery of cellular response to hypoxia in both GOBP and MsigDB datasets. It suggested that low pH could cause the same effects as hypoxia, which in turn is known to promote acidity, setting up a vicious cycle within the TME.

Interestingly, I also observed some contradictory terms in ORA enrichment results. For instance, both positive and negative regulation pathways of cell proliferation were enriched for myeloid and T cells. This inevitable limitation of enrichment analysis stems from the fact that it just takes into account whether a gene is present in the gene set of interest via hypergeometric test, ignoring factors such as the magnitude, direction (up- or down-regulated), or statistical significance of gene expression[154]. In addition, ORA analysis highly relies on pre-defined functional annotation databases, and the accuracy of enrichment findings might be impacted by their incompleteness. Although I used both GOBP and MsigDB datasets, there was still a lack of cascade effects or feedback loops for enrichment analysis of the upregulated gene set in response to low pH. Thus, we were only able to conclude from enrichment findings that certain biological pathways contributed to acidity response; but the direction of the pathway remained unknown.

To avoid such problems in pathway directions, I scored all 50 MsigDB Hallmark gene sets, compared between low and normal pH conditions, and visualized fold changes of 9 cancer-related pathways (Figure 4.1e). Each pathway score was determined by genes from each gene set with the *GSVA* function, and I subsequently

applied the package limma for condition comparison. While TNF-α signalling via NF-κB was suppressed in response to low pH, most cancer characteristic pathways were considerably enhanced at the transcriptome level across immune cells. This was consistent with previous studies showing that NF-κB activation would boost the generation of pro-inflammatory cytokines, and that its downregulation would promote immunological escape and apoptosis inside TME[155,156]. In addition, several acidity-related pathways like PI3K/AKT/mTOR signalling, glycolysis, adipogenesis, and the ROS pathway also showed elevated activity[18]. Furthermore, increased activity of Myc targets and DNA repair pathways was also identified as a response to chronic environmental stress, which inhibited the activity of immune activation regulators[157,158].

Nonetheless, because this GSVA scoring was only from the perspective of transcriptomics, validatory experiments, such as assessment for protein with western blotting, to confirm if the pathway was indeed up- or down-regulated at the protein level would be ideal next steps. For instance, IFN-γ signalling activity in our single-cell RNA-seq data was slightly elevated in response to environmental acidity. It seemed to be contradictory to our expectation that anti-tumour IFN-γ release should have been reduced within acidic TME. However, Pilon-Thomas et al.[102] had stated a plausible reason that IFN-γ release was not inhibited by an acidic pH at the transcriptomic level, suggesting that the impact of acidity might be post-translational. Quantitative RT-PCR showed that activated Pmel T cells cultured at pH 6.6 did not exhibit a significant difference in IFN-γ mRNA levels when compared to those at pH 7.4. Therefore, comparison of IFN-γ signalling activity was not 100% reliable with only gene expression profile. In brief, this scoring method was an additional reference with higher confidence, and wet lab experiments were further needed for final validation.

4.2 Time augments immune low-pH response

Given that PBMCs were cultured in both 4h and 24h groups, I applied DE analysis to investigate the effect of exposure time on transcriptomic response to low pH. Notably, due to varying statistical power in different sample sizes, the more cells we have, the more significant DE genes we get. In case of uneven distribution of cell populations between 4h and 24h conditions, I applied bootstrapping and downsampling in this case. Basically, each immune subset was downsampled to the stated number of cells for DE comparison between 4h and 24h conditions, and the linear mixed model $lmer(expr\ timepoint + (1|ID))$ was used across 50 bootstraps (Figure 4.2a). As expected, the median number of DE genes in 24h was greater than those of 4h groups across immune cells, for instance, at the number of 4,000 cells in DE comparison (Figure 4.2b). This suggested that low-pH exposure time enhanced immune transcriptomic response. Consistent with this finding from the standpoint of DE gene counts, fold change visualization of DE analysis in section 4.1 also showed that the average fold changes of 24h-specific genes were higher than those of 4h groups (Figure 4.1a). Thus, from perspectives of both significant DE gene numbers and fold changes, long-term exposure to environmental acidification would elevate immune transcriptomic response. Moreover, myeloid cells had the most intense transcriptomic response than T, B or NK cells (Figure 4.2a), which might imply myeloid cells have a higher sensitivity to extracellular low-pH stress and thus functionally dysregulated by an acidic TME.

Another fascinating issue was the effect of low-pH exposure time on biological pathways, that is, which signalling pathways become more active with long-term exposure. To solve it, I performed GOBP enrichment analysis across DE bootstraps. The heatmap visualized how many subsamples the pathway was found to be enriched out of 50 bootstraps (Figure 4.2c). Many enriched pathways, such

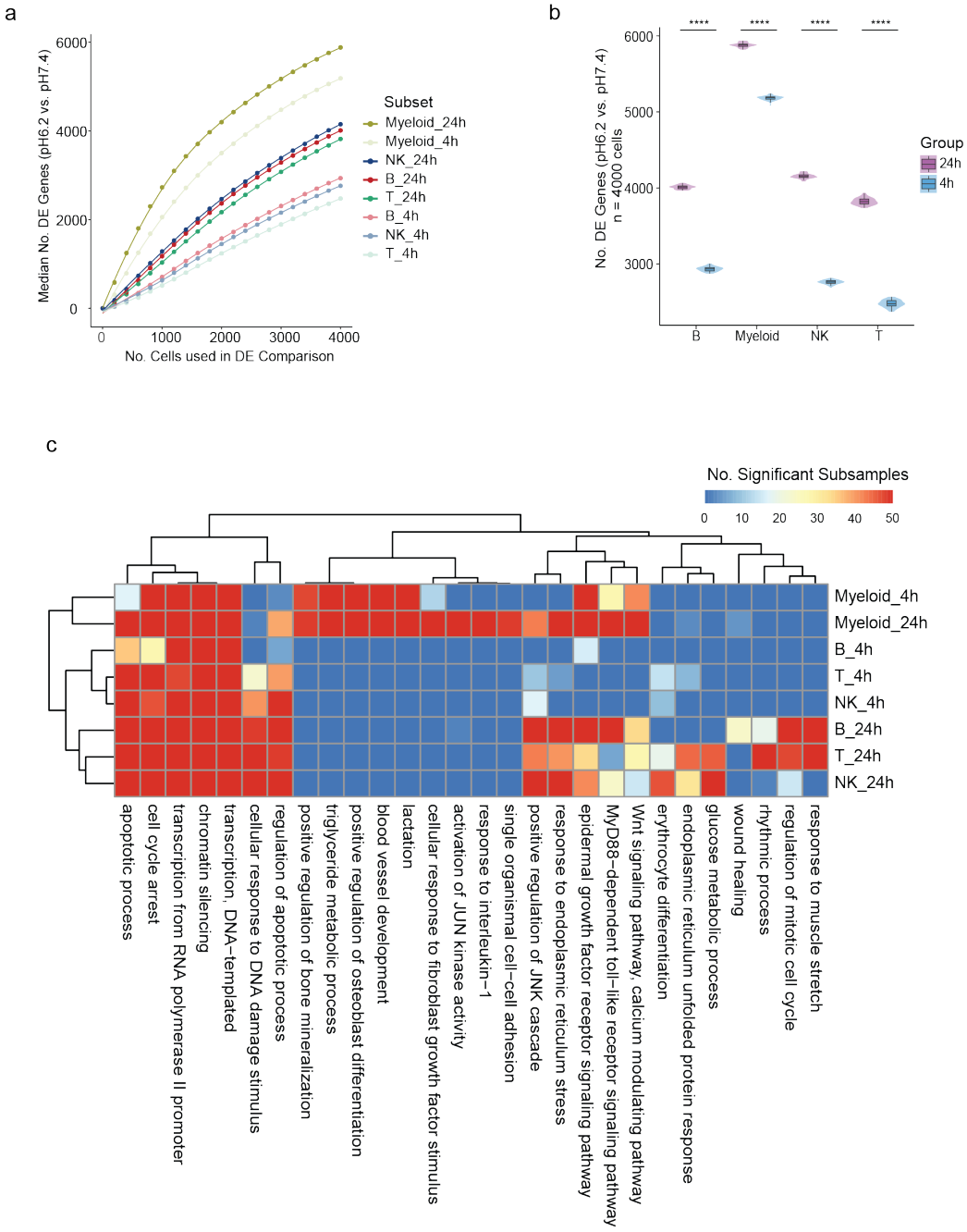

***Figure 4.2: Time augments transcriptomic response to low pH. a**, Linear graph showing the number of significant DE genes comparing between pH6.2 and pH7.4 for immune cells exposed to low pH for 4h and 24h, respectively. **b**, Boxplot of DE gene counts when downsampling each immune type at n=4,000 cells. **c**, Heatmap of GOBP pathways upregulated in low pH for each subset with colors representing how many subsamples were enriched.*

as the Wnt signalling, positive regulation of the JNK cascade, and endoplasmic reticulum (ER) stress - all established mechanisms in response to external stress - were time-sensitive in lymphoid cells. For instance, activated Wnt/β-catenin signalling might promote CTL exhaustion as well as Treg proliferation[159,160]. Also, JNK and ER stress were also related to continuous exposure to extracellular stress, lessening killing effects against tumour cells[161–163]. Conversely, myeloid cells exhibited pro-tumour characteristics that were elevated with long-term exposure to low pH, including response to IL-1, activation of JUN kinase activity and MyD88-dependent toll-like receptor (TLR) signalling. The increased degree of cell-cell adhesion was also identified, indicating potential immunosuppressive interactions between tumour-associated macrophages (TAMs) and cancer cells[164]. We also observed increased myeloid cell responsiveness to fibroblast growth factor (FGF) stimulus, which would facilitate the release of pro-angiogenic factors, like VEGF, within the TME[165]. All these enriched pathways indicated a higher likelihood of tumour progression and metastasis with prolonged exposure to acidity.

4.3 Conserved immune transcriptomic features

As stated beforehand, DE analysis might produce upregulated genes with minor biological variance, so I used high-dimensional weighted gene co-expression network analysis (hdWGCNA)[126] to identify hub genes that are critical in response to environmental acidosis. Instead of solely relying on variations in gene expression, hdWGCNA looks for core modules by analysing expression patterns and gene correlations, which highlights genes that are closely connected in the co-expression network. As a result, the genes found by hdWGCNA tend to be more specific and fewer in number; but they often represent a collection of genes involved in the same process, and indicate important regulatory mechanism that are

closely linked to low-pH response. Generally, hdWGCNA calculates gene-gene expression similarity by Pearson correlation, which is transformed into an adjacency matrix through soft thresholding. Following construction of a co-expression network, hierarchical clustering was performed to identify potential modules. We can then quantify the association between gene modules and the low-pH condition via Pearson correlation analysis, ultimately selecting one or more modules for further selection of hub genes.

Upon hdWGCNA analysis, I identified 4 potential gene modules that were positively related low extracellular pH. The scale-free networks were constructed for T, myeloid, NK and B cells, respectively. A total of 8 modules were found in myeloid cells, 5 in T cells, 2 in NK cells and 8 in B cells. With correlation analysis and hierarchical clustering, four modules from each immune subset were classified as low pH-responsive gene sets with strong positive association between acidic environments and gene modules - module 5 from myeloid cells (M-M5), module 4 from T cells (T-M4), module 2 from NK cells (NK-M2) and module 6 from B cells (B-M6) (Figure 4.3a). Based on eigengene connectivity within each module, top25 hub genes were visualized, including stress response-related genes (such as *HIST3H2A*, *HIST1H2AC*), hypoxia-induced genes (such as *HIF1A*) and tumour prognosis-associated genes (such as *HMGB2*, *THBS1*) (Figure 4.3b). In addition, AUCell scoring of these genes showed high expression in low pH-specific cell clusters, which cross-validated the positive relationship between microenvironmental acidosis and selected gene modules (Figure 4.3c).

Given that hdWGCNA did not take into account gene upregulation or downregulation between pH conditions, I overlapped hdWGCNA gene modules with DE genes within each immune subset, trying to obtain significant driver elements in response to low pH (Figure 4.3d). Subsequently, overlapping of acidity-induced

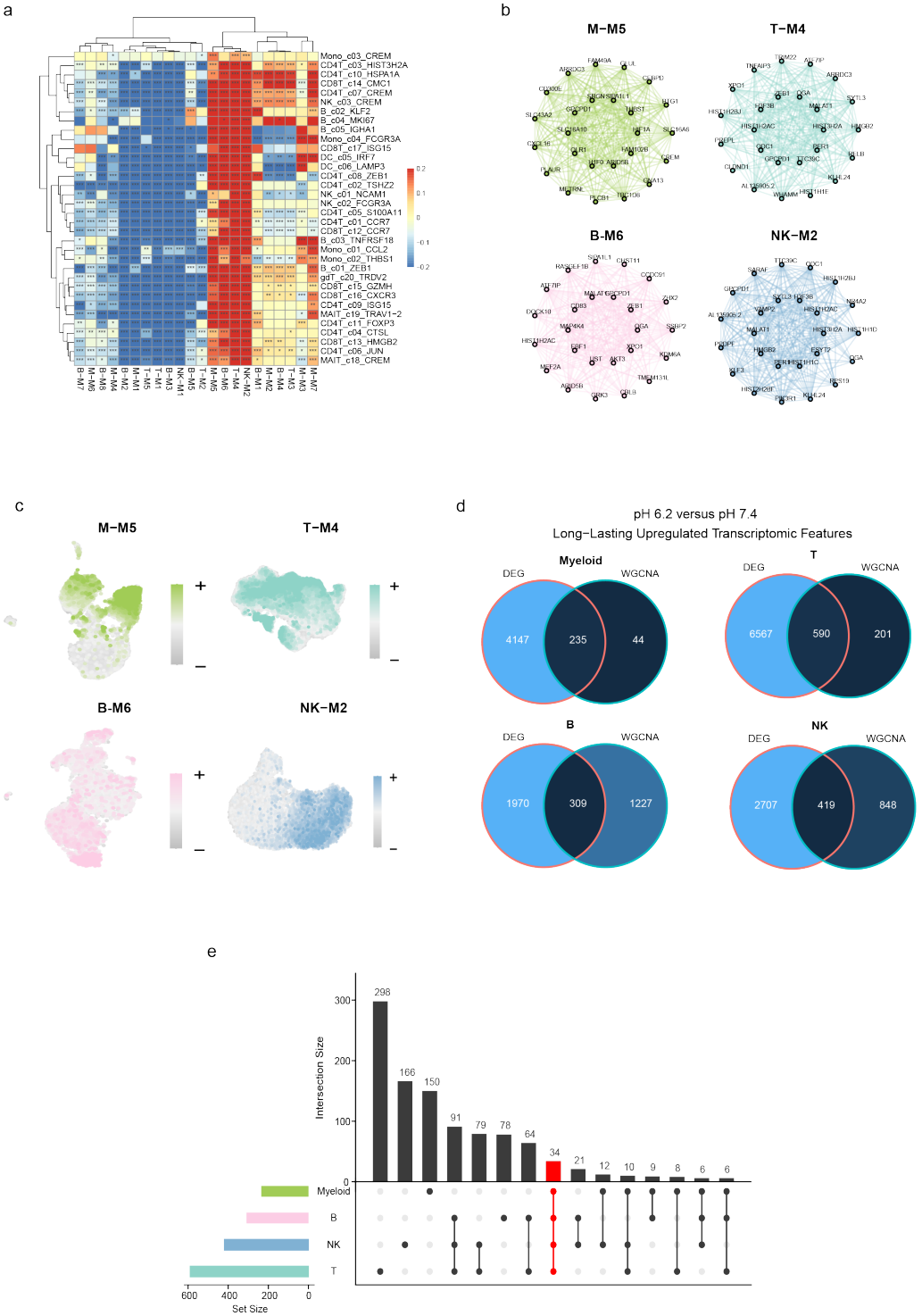
a
Mono_c03_CREM
CD4T_c03_HIST3H2A
CD4T_c10_HSPA1A
CD8T_c14_CMC1
CD4T_c07_CREM
NK_c03_CREM
B_c02_KLF2
B_c04_MKI67
B_c05_IGHA1
Mono_c04_FCGR3A
CD8T_c17_ISG15
DC_c05_IRF7
DC_c06_LAMP3
CD4T_c08_ZEB1
CD4T_c02_TSHZ2
NK_c01_NCAM1
NK_c02_FCGR3A
CD4T_c05_S100A11
CD4T_c01_CCR7
CD8T_c12_CCR7
B_c03_TNFRSF18
Mono_c01_CCL2
Mono_c02_THBS1
B_c01_ZEB1
gdT_c20_TRDV2
CD8T_c15_GZMH
CD8T_c16_CXCR3
CD4T_c09_ISG15
MAIT_c19_TRAV1-2
CD4T_c11_FOXP3
CD4T_c04_CTSL
CD8T_c13_HMGB2
CD4T_c06_JUN
MAIT_c18_CREM
B-M7 M-M6 B-M5 M-M4 B-M2 M-M1 T-M5 T-M1 B-M3 NK-M1 B-M1 M-M5 B-M6 T-M4 NK-M2 B-M1 M-M2 B-M4 T-M2 T-M3 M-M3 M-M7
0.2 0.1 0 -0.1 -0.2
b
M−M5
T−M4
B-M6
NK−M2
c
M−M5
T−M4
B-M6
NK−M2
d
pH 6.2 versus pH 7.4
Long−Lasting Upregulated Transcriptomic Features
Myeloid
DEG
WGCNA
4147
235
44
T
DEG
WGCNA
6567
590
201
B
DEG
WGCNA
1970
309
1227
NK
DEG
WGCNA
2707
419
848
e
Intersection Size
298
166
150
91
79
78
64
34
21
12
10
9
8
6
6
Myeloid
B
NK
T
600 400 200 0
Set Size

Figure 4.3: Conserved transcriptomic features across immune cells. ***a****, Heatmap of Pearson's association between hdWGCNA gene modules and pH conditions on each immune cell cluster. While red indicates positive correlation between gene modules and low pH, their negative relationships were demonstrated by blue. Hierarchical clustering was performed on each gene module.* ***b****, Connectivity network of top25 hub genes on pH-sensitive gene modules.* ***c****, Feature plot showing expression of top 25 hub genes on each selected module by UCell. All of them were highly expressed in low pH-specific cell clusters.* ***d****, Venn diagram of overlapped genes between pH-responsive WGCNA modules and DE genes that were significantly upregulated in both 4h and 24h time slots.* ***e****, Upset plot of cell type-specific pH-responsive genes, with the red bar showing conserved transcriptomic features in response to environmental acidosis.*

genes were performed among immune cells with the Upset plot (Figure 4.3e), with 34 genes identified as conserved transcriptomic signatures, including 1 rRNA gene and 33 protein-coding genes: *AC007384.1, ARRDC3, CCNG2, DDB2, DUSP1, ELL2, EMD, GADD45B, H1FX, H2AFJ, H3F3B, HIF1A, HIST1H1B, HIST1H1C, HIST1H1D, HIST1H1E, HIST1H2AC, HIST1H2AM, HIST1H2BC, HMGB2, KLF10, KLF3, NR4A2, PRDX6, PREPL, SAMSN1, SIPA1L1, STAT4, VAMP2, ZNF627, ZSCAN18, ZSWIM6, GPCPD1, RYBP*. To my expectation, almost half of the up-regulated genes were histone-related, which partly reflected epigenetic alterations during immune cell adaption to external acidic stress[166]. This might induce T-cell phenotypes of quiescence and exhaustion through chromatin remodelling when exposed to low pH stress[167]. Besides, the expression of the hypoxia TF HIF1A was also elevated in response to environmental acidosis, which suggested a loop feedback between low O_2 levels and H+ accumulation within the TME. Moreover, there were other conserved genes known as prognostic markers, such as HMGB2, which had been reported to promote radio-resistance in glioma via the base excision repair pathway, as well as sustain exhausted CD8+ T differentiation and stemness within the TME[135–137]. In summary, in combination of hdWGCNA and DE analysis, I found a set of low pH-responsive genes that might play a crucial role in immunosuppression and metabolite reprogramming.

4.4 Cross-validation of pH-responsive features

Upon identification of conserved transcriptomic signatures in response to acidic environments, a key question emerged regarding their potential applications in anti-tumour therapies. Therefore, I leveraged the bulk RNA-seq database, CellMiner, to investigate how immune cells affect drug sensitivity. Intriguingly, certain medications, like lanvatinib, showed a positive correlation with pH-responsive signatures, whereas other compounds, such as PD-185352, displayed an adverse relationship with the acidification of the environment (Figure 4.4).

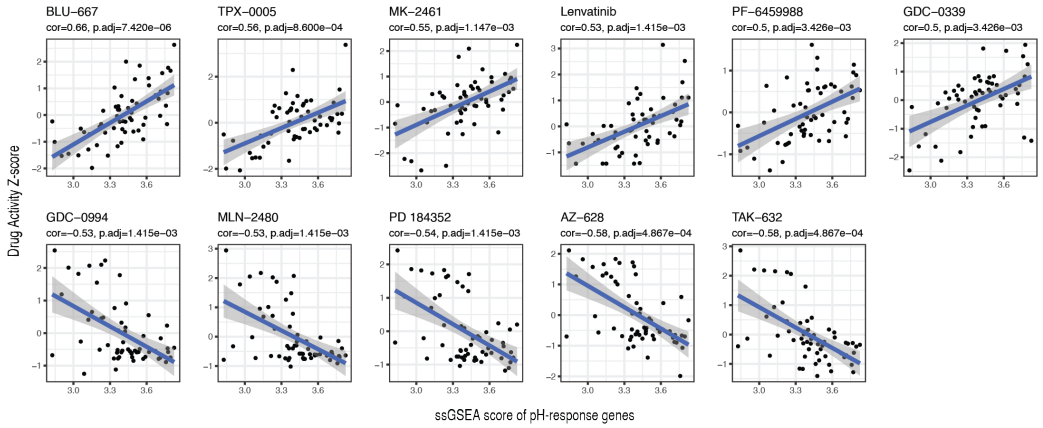

Figure 4.4: Cross-validation of pH-responsive features with CellMiner. *This figure panel demonstrated drug sensitivity in response to low pH. Conserved pH-sensitive genes were scored by ssGSEA and correlated with CellMiner drug activity z-scores via the generalized linear model.*

These findings raised plausible speculations about drug mechanisms in the context of environmental acidosis. Chemotherapy and/or targeted drugs that were positively associated with pH-responsive gene expression might improve immune cell activation, proliferation, or cytokine release via inhibiting low-pH targets, which would increase their anti-tumour ability; conversely, resistance to these negatively

correlated drugs might involve immune escape mechanisms or pathways leading to immune cell exhaustion, reducing the effectiveness of therapy. By utilizing this conserved low pH-specific gene set, we offered a practical method for assessing a drug's suitability through peripheral blood transcriptomics analysis. But these discoveries were only based on the connection between bulk RNA-seq data and single cell-derived gene sets, necessitating further experimental validation. Future studies could focus on verifying the impact of these positively and negatively correlated drugs on specific immune cell functions, such as cytokine production, cytotoxicity in targeted cell assays. This would provide deeper insights into how environmental acidosis shapes drug sensitivity through immune modulation.

5 | GPR65 genotype heterogeneity involved in acidic environments

5.1 The effect of rs3742704 on transcriptomic response to acidity

As a proton-sensing G-protein coupled receptor, GPR65 has been reported to play a critical role in a variety of physiological and pathological pathways by sensing extracellular acidic conditions, especially in the context of autoimmunity and TME[168–171]. For example, GPR65 acts as a novel regulator of helper T cell differentiation from CD4+ T cells to Th1/Th17 cells in inflammatory bowel diseases[168], as well as results in high metastatic rates and poor patients' outcomes in osteosarcoma[171]. In addition, GPR65 was also identified as the hub gene of M2 macrophage-related module by WGCNA analysis, which constituted the immunosuppressive TME in glioma[169]. Considering the sensitivity of GPR65 to low pH, its implicated role in modulating immune responses and importance within acidic TME, I studied the impact of rs3742704, a GPR65 single nucleotide polymorphism (SNP) that reduces the effect of GPR65 activity (hypomorphic), on transcriptomic response to environmental low pH. The aim of this approach was to see if we could leverage genetics to infer the role of GPR65 in the response to low pH in the TME. This was in keeping with one of the original aims of the collaboration between the Fairfax group and Pathios Therapeutics.

To investigate the effects of GPR65 genotype heterogeneity on transcriptomic response to low pH, I applied similar downsampling and bootstrapping across GPR65 SNP rs3742704 carriers and non-carriers as stated in section 4.2. In our

single-cell dataset, there were 7 non-carriers, 3 heterozygotes for minor hypomorphic allele and 2 homozygous for this allele. Each immune subset was split into carriers and non-carriers, and subsequently downsampled into indicated number of cells across 50 bootstraps. Interestingly, in myeloid cells, rs3742704 carriers showed increased number of DE genes in comparison to non-carriers, whereas rs3742704 reduced the transcriptomic response to low pH in NK, T and B cells (Figure 5.1a-b). These results are intriguing, but would be consistent with a model where GPR65 activity contributed to the transcriptomic response to pH. Such a distinct response between lymphoid and myeloid cells was unexpected, and could be interpreted as cell type-specific transcriptomic alterations induced by the rs3742704 polymorphism. Ideally we shall attempt to replicate this is a further cohort of samples, but recruiting further individuals with the rare alelel was outside the timeframe of this thesis.

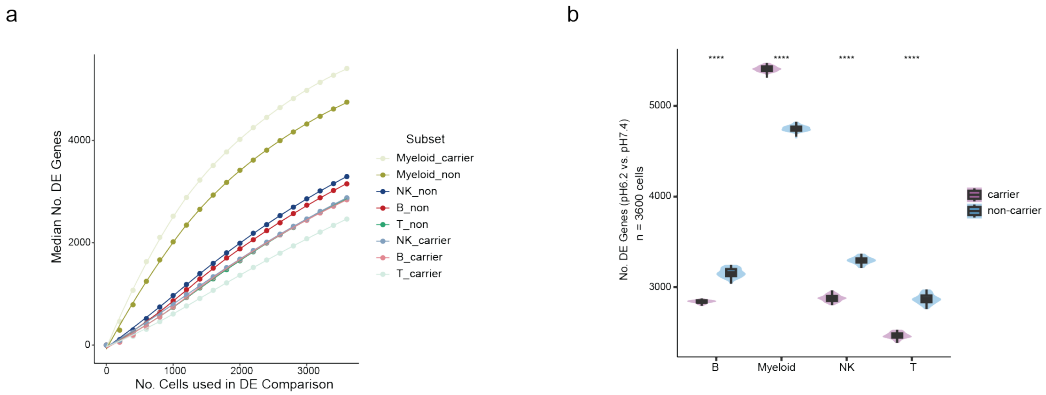

Figure 5.1: The effect of rs3742704 on transcriptomic response to acidity. *a, Linear graph showing the number of significant DE genes for immune subsets with or without rs3742704. Each immune subset was downsampled to the indicated number of cells, and DE analysis was applied comparing pH 6.2 and pH 7.4. b, Boxplot of DE gene counts when downsampling each immune type at n=3,600 cells. The rs3742704 carriers had significantly larger numbers of DE genes than non-carriers across immune cells.*

5.2 GPR65 module score

Given the difference of rs3742704 transcriptomic effects between myeloid and lymphoid cells, I next established a GPR65 module score to determine whether or not GPR65 signalling showed distinct response to environmental acidosis between them. With the Stringdb database, protein-protein interaction (PPI) network analysis was performed focusing on GPR65, which generated 10 closely correlated genes (Figure 5.2a). Subsequently, I tested gene-gene association between GPR65 and these 10 genes in our single-cell data (Figure 5.2b). To my expectation, all of them were positively related to GPR65. Although 4 out of 10 were not significant, this might result from single-cell data sparsity. Next, I calculated UCell scores for T, B, NK and myeloid cells between pH 6.2 and pH 7.4; interestingly, extracellular low pH significantly augmented GPR65 signalling activity in lymphoid cells, while it is conversely inhibited in myeloid cells (Figure 5.2c). This was consistent with the genotyping result as shown before, which suggested that the GPR65 had a cell type-specific regulatory mechanism in response to acidity.

A possible explanation would be that acidosis-induced GPR65 signaling inhibits immune response against tumours, where the SNP rs3742704 lessens GPR65 activity by changing its protein structure. In response to low pH, GPR65 shows cell type-specific response that are elevated in lymphoid cells but inhibited in myeloid cells. This is congruent with previous publications indicating GPR65 as an immune checkpoint within the TME, associating with poor prognosis via pan-cancer analysis[170]. Notably, certain myeloid cells, like tumour-associated macrophages, appear to be most influenced by the acidic TME to promote tumour development – as here I show that the monocyte response includes induction of pro-angiogenic genes such as *VEGF*. Furthermore, the SNP rs3742704 may alter the protein's conformational shape, reduce its binding affinity, and lessen the activation or in-

hibition of GPR65 activity caused by low pH. However, the molecular mechanism underlying cell type-specific response of GPR65 to low pH still remains unclear – it might relate to expression differences of the GPR65 or of downstream regulatory network genes that transduce the GPR65 signal.

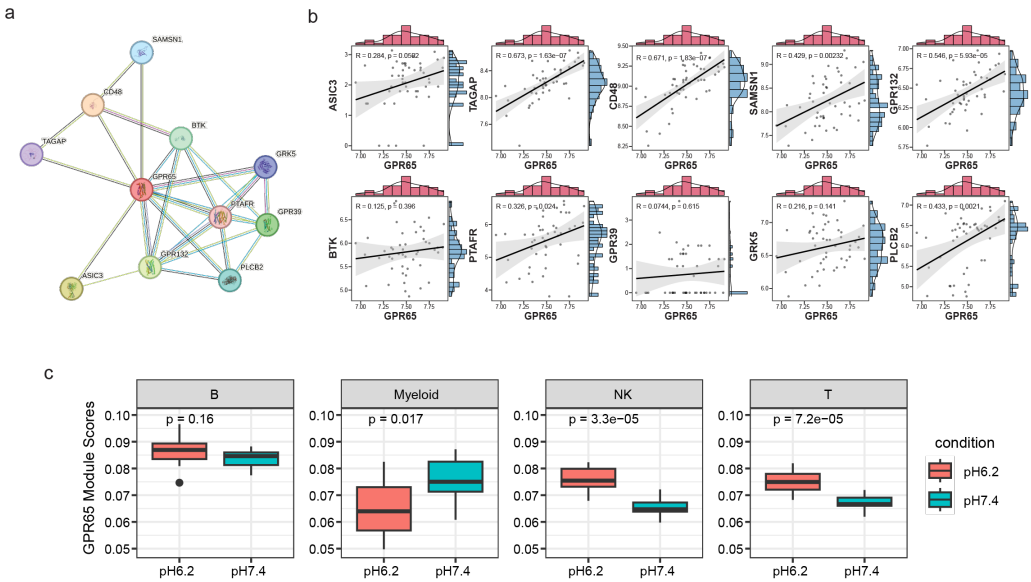

Figure 5.2: GPR65 module score. *a, Protein-Protein Interaction (PPI) network obtained from the String_v12.0 database. b, Scatter plot showing pseudobulk-level association between GPR65 expression and other 10 genes from PPI analysis. All 10 genes were positively correlated, and they were used as a GPR65 module for scoring. c, Boxplot comparing UCell scores of the GPR65 module between pH6.2 and pH7.4.*

6 | Discussion and Conclusion

6.1 Overall Summary

In this project I have described and analysed the first single-cell transcriptomic assessment of the response to environmental low pH among peripheral blood mononuclear cells. The work acts as a novel reference for investigating acidic environments involved in physiological and/or pathological processes, such as wound healing, deep infections and the TME. The work has identified pH-sensitive cell subtypes in terms of changes in numbers and transcriptional profiles contrasting low and normal pH conditions. I have subsequently used the bioinformatic tools SCENIC and hdWGCNA to further define the gene regulatory networks, including dissection of TF regulons and pH-responsive gene modules. This approach allows one to move from simple lists of differentially regulated genes, towards better understanding of the complex transcriptomic consequences and potential drivers of these. The work shows that the low pH environment of the TME can be envisaged to have distinct effects across different cell subsets – most notably, I find a pronounced induction of pro-angiogenic pathways in myeloid cells driven directly via low extracellular pH.

The identified immune cell clusters and transcriptomic features provide promising targets for drug discovery and I use approaches to identify potential modulators of the pH response. Metabolic signatures within the TME, such as cellular response to glycolysis, adipogenesis and hypoxia, are replicated in healthy PBMCs after being solely exposed to acidity. This suggests that extracellular low pH might interact with other metabolites within the TME, forming a vicious feedback loop. In addition to metabolite reprogramming, immune cells also respond to extracellular acidification by altering immune-related transcriptomics. Within an acidic envi-

ronment, immune cells exhibits numerous immunosuppressive features (such as angiogenesis and TP53-related apoptosis) that are comparable to those within the TME. These signatures also provides additional evidence that low pH can induce cell exhaustion, chronic inflammation as well as immune escape.

Finally, I have investigated the effect of a rare coding polymorphism - rs3742704 – in GPR65 which encodes a pH sensitive G protein coupled receptor of the same name to explore the function of this gene in the pH response. The SNP rs3742704 leads to hypomorphic activity - corresponding to reduced function – of GPR65. Using this SNP I show that reduced activity of this gene has potentially opposing effects of gene expression on lymphoid and myeloid cells in their response to environmental acidification. I subsequently established a GPR65 module score identifying a group of genes co-regulated with GPR65 for further investigation. This provides another dimension of genotyping profile on low-pH response.

6.2 Limitations of the study

Despite the novelty of this study, there are still some potential limitations that require further improvements. Cultured immune cells from PBMCs are not identical to those found in the TME. Primarily, these cells are from healthy people without cancer. Further, the tumour microenvironment is a relative stable tissue with gradual decreases of pH, whereas our cell culture exposed PBMCs switch to pH 6.2 abruptly, - many stress response-related genes would be up-regulated with extreme fold changes likely in excess of those in the pathophysiological state. Whilst this approach ensures we make observations, it might be better to sequence PBMCs exposed to a series of extracellular pH values. Meanwhile, cell types are not exactly the same between peripheral blood and tissue-resident immune cells. Take DCs as an example, where there is only a small proportion of peripheral blood

DCs in comparison tissue-resident ones. In order to better recapitulate pathophysiological processes induced by environmental acidification, it is recommended to sort and culture immune cells isolated from tissue biopsies, such as skin cells. With tissue culture, more cell types could be taken into account to mimic the acidic TME. Integration of tumour immune samples, para-tumour normal tissues and peripheral blood might be an additional way to compare between cancer patients and healthy donors. Moreover, the immune cell culture duration should be extended, and the protocol has to be improved; but the biggest challenge is that 24 hours of culture under low pH conditions might lead to a substantial cell death rate. Thus, it is worthwhile to investigate how to minimize the long-term effects of excessive cell death on sequencing quality. 24h exposure in this study only reflects relative long-term cellular adaptation to acidity, but the transcriptomic response under more prolonged exposure to low pH remains unknown.

In addition to possible limitations during sample preparation, we must not overlook potential problems in data analysis. The limited space used for cultivating immune cells differs from a circulating system, which might result in confounding factors. Compared with conventional PBMCs, the transcriptome profile of low-pH simulated cells is more complex, with certain cell clusters lacking recognized functional markers. It is challenging to exclude these confounding elements, as the profile may be governed by a multitude of stress factors. Besides, due to single-cell data sparsity, it is unavoidable to obtain false negative features in response to low pH. This issue might be resolved by multi-modal integration of spatial transcriptomics and/or bulk RNA-seq, cross-validating the conserved pH-responsive gene set derived from our data. Moreover, interstitial acidosis is also related to other non-cancerous diseases, including infection, ischemia, inflammatory disorders as well as systemic respiratory abnormalities, which indicates that low pH is implicated in multitude of pathophysiological processes[172,173].

6.3 Future Perspectives

Given that conserved transcriptomic features were identified among immune cells, my initial plan would be to verify this low pH-specific gene collection using bulk RNA-seq. With immune cells sorted from TME of multiple cancer types, I can score conserved signatures through average expression, and perform survival analysis associating this gene set with patients' outcome. Besides, by cell deconvolution, low pH-specific cell clusters could also be inferred in bulk data for cross-validation. In addition, T-cell clonality dynamics can be studied with regards to pH changes. By comparing T cells between persistent and shrinkable clones, I am able to obtain VDJ information in addition to transcriptomic profile. Also, scoring of known cytotoxicity-related genes is another option for T cell clones of interest, which assists in phenotype identification of clones.

It is helpful if we integrate proteomics data with this single-cell transcriptomics atlas, like CITE-seq[174] that detects both RNA and cell surface proteins in an unbiased manner. Ideally, I would like to identify surface markers of low pH exposure for potential tracking in the circulation -this would be the first step towards such work. The gene expression profile derived from scRNA-seq can only represent information at the mRNA level instead of protein-level portraits. Similar results cannot be explained if certain alterations occur on the post-translational side. IFN-γ signalling is a representative example as stated above, where low pH decreases IFN-γ at the protein level, but does not significantly alter gene expression[102].

This project mainly studies overlapped genes between 4h and 24h, but 4h-specific and 24h-specific DE genes are also an issue worth exploring. What exactly causes certain genes to downregulate after chronic exposure to low pH? What is the role of genes that did not change significantly before but appeared later? Which path-

ways are more sensitive with low-pH exposure time increasing? To study these problems, it is recommended to use bulk RNA-seq with more sequencing depth.

There is still a lack of wet lab experiments to cross-validate these bioinformatics findings. The single-cell profile only provides us with a transcriptomic reference with potential directions to focus. For instance, we are able to conduct co-culturing of tumour and immune cells to analyse how acidity affects the cytotoxic effects of immune cells against solid tumours. By inhibiting or activating specific signalling pathways, we can verify the functional role of pH-responsive gene sets under acidic conditions.

6.4 Conclusion

Tumours, according to Harold Dvorak[175], are wounds that do not heal. This is a classic notion that is quite suitable in the context of environmental low pH. Temporary tissue acidity is commonly involved in wound response that fades away when the lesion heals. In contrast, the extracellular acidosis never resolves in the TME, which formed an acidic wound that never 'heals'. Albeit earlier findings of immune escape driven by acidic TME, we have described how immune cells might be regulated by low pH from the perspective of whole transcriptomics. Notably, unlike other single-cell sequencing studies of TME, we have isolated pH as an independent variable and studied the effects of environmental acidity on immune cells. This provides a comprehensive atlas targeting low pH for novel drug discovery targeting extracellular acidity.

7 | Appendix

7.1 Softwares and Algorithms

Packages	Authors	Sources
bcftools v1.17	Danecek et al.[176]	https://github.com/samtools/bcftools
CellRanger v7.1.0	Zheng et al.[114]	https://10xgenomics.com/
cellsnp-lite v1.2.0	Huang et al.[116]	https://github.com/single-cell-genetics/cellsnp-lite
DoubletFinder v2.0.3	McGinnis et al.[120]	https://github.com/chris-mcginnis-ucsf/DoubletFinder
DropletUtils v1.20.0	Lun et al.[115]	https://github.com/MarioniLab/DropletUtils
Harmony v1.0.3	Korsunsky et al.[133]	https://github.com/immunogenomics/harmony
hdWGCNA v0.2.27	Morabito et al.[126]	https://github.com/smorabit/hdWGCNA
limma v3.56.1	Ritchie et al.[177]	https://github.com/cran/limma
plink v1.90	Chang et al.[178]	https://www.cog-genomics.org/plink/
R v4.3.0	R Core Team[179]	https://www.r-project.org/
pySCENIC v0.12.2	Aibar et al.[127]	https://github.com/aertslab/SCENIC

Packages	Authors	Sources
Seurat v4.3.0	Hao et al.[122]	https://github.com/satijalab/seurat
scDblFinder v1.14.0	Germain et al.[118]	https://github.com/plger/scDblFinder
scrublet v0.2.3	Wolock et al.[119]	https://github.com/swolock/scrublet
singleR v2.2.0	Aran et al.[180]	https://github.com/dviraran/SingleR
soupX v1.6.2	Young et al.[121]	https://github.com/constantAmateur/SoupX
vcftools 0.1.16	Danecek et al.[181]	https://github.com/vcftools/vcftools
vireo v0.2.3	Huang et al.[117]	https://github.com/single-cell-genetics/vireo
XGR v1.1.9	Fang et al.[182]	https://xgr.r-forge.r-project.org/

7.2 Table of pooled cell numbers by deconvolution of genotyping data

HD	816	817	818	819	820	821	822
P1	3283	3040	3472	3569	2938	3145	4053
P2	2655	2835	2929	3200	3078	3473	3322
P3	2659	2590	3262	2790	3271	3170	2548
P4	3056	3703	3090	3105	3502	3925	3796
P5							
P6							
P7							
P8							

HD	823	824	825	826	827	doub	unk
P1	3923					6130	622
P2	4095					6584	1753
P3	2914					4662	562
P4	3060					5730	848
P5		2776	3179	2584	2717	4929	351
P6		2988	3225	3783	2203	4236	337
P7		1993	2633	2092	1800	4701	305
P8		3168	2898	3728	2011	4114	444

HD, healthy donor; 816-827, individual tags; P1-P8, Pool1-Pool8; doub, doublet; unk, unknown.

Bibliography

1. De Visser, K. E. & Joyce, J. A. The evolving tumor microenvironment: From cancer initiation to metastatic outgrowth. *Cancer Cell* **41,** 374–403 (2023).
2. Jin, M.-Z. & Jin, W.-L. The updated landscape of tumor microenvironment and drug repurposing. *Signal Transduction and Targeted Therapy* **5,** 166 (2020).
3. Binnewies, M., Roberts, E. W., Kersten, K., *et al.* Understanding the tumor immune microenvironment (TIME) for effective therapy. *Nature Medicine* **24,** 541–550 (2018).
4. *Nobel Prize in Physiology or Medicine 2018* https://www.nature.com/collections/gqznlfngkz (2024).
5. Waldman, A. D., Fritz, J. M. & Lenardo, M. J. A guide to cancer immunotherapy: from T cell basic science to clinical practice. *Nature Reviews Immunology* **20,** 651–668 (2020).
6. Larkin, J., Chiarion-Sileni, V., Gonzalez, R., *et al.* Five-Year Survival with Combined Nivolumab and Ipilimumab in Advanced Melanoma. *New England Journal of Medicine* **381,** 1535–1546 (2019).
7. Wolchok, J. D., Chiarion-Sileni, V., Gonzalez, R., *et al.* Overall Survival with Combined Nivolumab and Ipilimumab in Advanced Melanoma. *New England Journal of Medicine* **377,** 1345–1356 (2017).
8. Tiwari, A., Trivedi, R. & Lin, S.-Y. Tumor microenvironment: barrier or opportunity towards effective cancer therapy. *Journal of Biomedical Science* **29,** 83 (2022).

9. Zheng, R., Li, F., Li, F. & Gong, A. Targeting tumor vascularization: promising strategies for vascular normalization. *Journal of Cancer Research and Clinical Oncology* **147,** 2489–2505 (2021).
10. Fang, J., Lu, Y., Zheng, J., *et al.* Exploring the crosstalk between endothelial cells, immune cells, and immune checkpoints in the tumor microenvironment: new insights and therapeutic implications. *Cell Death & Disease* **14,** 586 (2023).
11. Li, C., Jiang, P., Wei, S., Xu, X. & Wang, J. Regulatory T cells in tumor microenvironment: new mechanisms, potential therapeutic strategies and future prospects. *Molecular Cancer* **19,** 116 (2020).
12. Ihara, F., Sakurai, D., Takami, M., *et al.* Regulatory T cells induce CD4- NKT cell anergy and suppress NKT cell cytotoxic function. *Cancer Immunology, Immunotherapy* **68,** 1935–1947 (2019).
13. Dysthe, M. & Parihar, R. in *Tumor Microenvironment: Hematopoietic Cells – Part A* (ed Birbrair, A.) 117–140 (Springer International Publishing, Cham, 2020).
14. Liu, T., Han, C., Wang, S., *et al.* Cancer-associated fibroblasts: an emerging target of anti-cancer immunotherapy. *Journal of Hematology & Oncology* **12,** 86 (2019).
15. Winkler, J., Abisoye-Ogunniyan, A., Metcalf, K. J. & Werb, Z. Concepts of extracellular matrix remodelling in tumour progression and metastasis. *Nature Communications* **11,** 5120 (2020).
16. Toor, S. M., Sasidharan Nair, V., Decock, J. & Elkord, E. Immune checkpoints in the tumor microenvironment. *Seminars in Cancer Biology* **65,** 1–12 (2020).

17. Wu, X., Li, T., Jiang, R., *et al.* Targeting MHC-I molecules for cancer: function, mechanism, and therapeutic prospects. *Molecular Cancer* **22,** 194 (2023).

18. Boedtkjer, E. & Pedersen, S. F. The Acidic Tumor Microenvironment as a Driver of Cancer. *Annual Review of Physiology* **82,** 103–126 (2020).

19. Huber, V., Camisaschi, C., Berzi, A., *et al.* Cancer acidity: An ultimate frontier of tumor immune escape and a novel target of immunomodulation. *Seminars in Cancer Biology* **43,** 74–89 (2017).

20. Estrella, V., Chen, T., Lloyd, M., *et al.* Acidity Generated by the Tumor Microenvironment Drives Local Invasion. *Cancer Research* **73,** 1524–1535 (2013).

21. Brand, A., Singer, K., Koehl, G. E., *et al.* LDHA-Associated Lactic Acid Production Blunts Tumor Immunosurveillance by T and NK Cells. *Cell Metabolism* **24,** 657–671 (2016).

22. Chiche, J., Brahimi-Horn, M. C. & Pouysségur, J. Tumour hypoxia induces a metabolic shift causing acidosis: a common feature in cancer. *Journal of Cellular and Molecular Medicine* **14,** 771–794 (2010).

23. Wu, H., Ying, M. & Hu, X. Lactic acidosis switches cancer cells from aerobic glycolysis back to dominant oxidative phosphorylation. *Oncotarget* **7,** 40621–40629 (2016).

24. Rohani, N., Hao, L., Alexis, M. S., *et al.* Acidification of Tumor at Stromal Boundaries Drives Transcriptome Alterations Associated with Aggressive Phenotypes. *Cancer Research* **79,** 1952–1966 (2019).

25. Helmlinger, G., Yuan, F., Dellian, M. & Jain, R. K. Interstitial pH and pO2 gradients in solid tumors in vivo: High-resolution measurements reveal a lack of correlation. *Nature Medicine* **3,** 177–182 (1997).

26. Gillies, R. J., Brown, J. S., Anderson, A. R. A. & Gatenby, R. A. Eco-evolutionary causes and consequences of temporal changes in intratumoural blood flow. *Nature Reviews Cancer* **18,** 576–585 (2018).

27. Vander Heiden, M. G., Cantley, L. C. & Thompson, C. B. Understanding the Warburg Effect: The Metabolic Requirements of Cell Proliferation. *Science* **324,** 1029–1033 (2009).

28. Liberti, M. V. & Locasale, J. W. The Warburg Effect: How Does it Benefit Cancer Cells? *Trends in Biochemical Sciences* **41,** 211–218 (2016).

29. Stine, Z. E., Schug, Z. T., Salvino, J. M. & Dang, C. V. Targeting cancer metabolism in the era of precision oncology. *Nature Reviews Drug Discovery* **21,** 141–162 (2022).

30. Ganapathy-Kanniappan, S. & Geschwind, J.-F. H. Tumor glycolysis as a target for cancer therapy: progress and prospects. *Molecular Cancer* **12,** 152 (2013).

31. Chen, S., Xu, Y., Zhuo, W. & Zhang, L. The emerging role of lactate in tumor microenvironment and its clinical relevance. *Cancer Letters* **590,** 216837 (2024).

32. Emami Nejad, A., Najafgholian, S., Rostami, A., *et al.* The role of hypoxia in the tumor microenvironment and development of cancer stem cell: a novel approach to developing treatment. *Cancer Cell International* **21,** 62 (2021).

33. Masson, N. & Ratcliffe, P. J. Hypoxia signaling pathways in cancer metabolism: the importance of co-selecting interconnected physiological pathways. *Cancer Metabolism* **2,** 3 (2014).

34. Infantino, V., Santarsiero, A., Convertini, P., Todisco, S. & Iacobazzi, V. Cancer Cell Metabolism in Hypoxia: Role of HIF-1 as Key Regulator and

Therapeutic Target. *International Journal of Molecular Sciences* **22,** 5703 (2021).

35. Lee, S.-H. & Griffiths, J. R. How and Why Are Cancers Acidic? Carbonic Anhydrase IX and the Homeostatic Control of Tumour Extracellular pH. *Cancers* **12,** 1616 (2020).
36. Hu, Y., Lou, J., Jin, Z., *et al.* Advances in research on the regulatory mechanism of NHE1 in tumors (Review). *Oncology Letters* **21,** 273 (2021).
37. Flinck, M., Kramer, S. H., Schnipper, J., Andersen, A. P. & Pedersen, S. F. The acid-base transport proteins NHE1 and NBCn1 regulate cell cycle progression in human breast cancer cells. *Cell Cycle* **17,** 1056–1067 (2018).
38. Flinck, M., Hagelund, S., Gorbatenko, A., *et al.* The Vacuolar H+ ATPase α3 Subunit Negatively Regulates Migration and Invasion of Human Pancreatic Ductal Adenocarcinoma Cells. *Cells* **9,** 465 (2020).
39. Sennoune, S. R., Bakunts, K., Martínez, G. M., *et al.* Vacuolar H-ATPase in human breast cancer cells with distinct metastatic potential: distribution and functional activity. *American Journal of Physiology-Cell Physiology* **286,** C1443–C1452 (2004).
40. Corbet, C. & Feron, O. Tumour acidosis: from the passenger to the driver's seat. *Nature Reviews Cancer* **17,** 577–593 (2017).
41. Payen, V. L., Mina, E., Van Hée, V. F., Porporato, P. E. & Sonveaux, P. Monocarboxylate transporters in cancer. *Molecular Metabolism* **33,** 48–66 (2020).
42. Endeward, V., Al-Samir, S., Itel, F. & Gros, G. How does carbon dioxide permeate cell membranes? A discussion of concepts, results and methods. *Frontiers in Physiology* **4** (2014).
43. Lee, S., Mele, M., Vahl, P., *et al.* Na+,HCO3 –cotransport is functionally upregulated during human breast carcinogenesis and required for the in-

verted pH gradient across the plasma membrane. *Pflügers Archiv - European Journal of Physiology* **467,** 367–377 (2015).

44. Pamarthy, S., Kulshrestha, A., Katara, G. K. & Beaman, K. D. The curious case of vacuolar ATPase: regulation of signaling pathways. *Molecular Cancer* **17,** 41 (2018).
45. Voss, N. C. S., Kold-Petersen, H., Henningsen, M. B., Homilius, C. & Boedtkjer, E. Upregulated Na+/H+-Exchange Protects Human Colon Cancer Tissue against Intracellular Acidification. *BioMed Research International* **2019,** 1–5 (2019).
46. Hanahan, D. & Weinberg, R. A. Hallmarks of Cancer: The Next Generation. *Cell* **144,** 646–674 (2011).
47. Morita, T., Nagaki, T., Fukuda, I. & Okumura, K. Clastogenicity of low pH to various cultured mammalian cells. *Mutation Research/Fundamental and Molecular Mechanisms of Mutagenesis* **268,** 297–305 (1992).
48. Xiao, H., Li, T.-K., Yang, J.-M. & Liu, L. F. Acidic pH induces topoisomerase II-mediated DNA damage. *Proceedings of the National Academy of Sciences* **100,** 5205–5210 (2003).
49. Massonneau, J., Ouellet, C., Lucien, F., *et al.* Suboptimal extracellular pH values alter DNA damage response to induced double-strand breaks. *FEBS Open Bio* **8,** 416–425 (2018).
50. Flinck, M., Kramer, S. H. & Pedersen, S. F. Roles of pH in control of cell proliferation. *Acta Physiologica* **223,** e13068 (2018).
51. Shi, Q., Maas, L., Veith, C., Van Schooten, F. J. & Godschalk, R. W. Acidic cellular microenvironment modifies carcinogen-induced DNA damage and repair. *Archives of Toxicology* **91,** 2425–2441 (2017).
52. Bernards, R. & Weinberg, R. A. Metastasis genes: A progression puzzle. *Nature* **418,** 823–823 (2002).

53. Moellering, R. E., Black, K. C., Krishnamurty, C., *et al.* Acid treatment of melanoma cells selects for invasive phenotypes. *Clinical & Experimental Metastasis* **25,** 411–425 (2008).

54. Zhang, H. Y., Hormi-Carver, K., Zhang, X., Spechler, S. J. & Souza, R. F. In Benign Barrett's Epithelial Cells, Acid Exposure Generates Reactive Oxygen Species That Cause DNA Double-Strand Breaks. *Cancer Research* **69,** 9083–9089 (2009).

55. Plaks, V., Kong, N. & Werb, Z. The Cancer Stem Cell Niche: How Essential Is the Niche in Regulating Stemness of Tumor Cells? *Cell Stem Cell* **16,** 225–238 (2015).

56. Hu, P., Li, S., Tian, N., *et al.* Acidosis enhances the self-renewal and mitochondrial respiration of stem cell-like glioma cells through CYP24A1-mediated reduction of vitamin D. *Cell Death & Disease* **10,** 25 (2019).

57. Filatova, A., Seidel, S., Böğürcü, N., *et al.* Acidosis Acts through HSP90 in a PHD/VHL-Independent Manner to Promote HIF Function and Stem Cell Maintenance in Glioma. *Cancer Research* **76,** 5845–5856 (2016).

58. Hjelmeland, A. B., Wu, Q., Heddleston, J. M., *et al.* Acidic stress promotes a glioma stem cell phenotype. *Cell Death & Differentiation* **18,** 829–840 (2011).

59. Andreucci, E., Peppicelli, S., Ruzzolini, J., *et al.* The acidic tumor microenvironment drives a stem-like phenotype in melanoma cells. *Journal of Molecular Medicine* **98,** 1431–1446 (2020).

60. Egeblad, M. & Werb, Z. New functions for the matrix metalloproteinases in cancer progression. *Nature Reviews Cancer* **2,** 161–174 (2002).

61. Kato, Y., Lambert, C. A., Colige, A. C., *et al.* Acidic Extracellular pH Induces Matrix Metalloproteinase-9 Expression in Mouse Metastatic Melanoma

Cells through the Phospholipase D-Mitogen-activated Protein Kinase Signaling. *Journal of Biological Chemistry* **280,** 10938–10944 (2005).

62. Rastogi, S., Mishra, S. S., Arora, M. K., *et al.* Lactate acidosis and simultaneous recruitment of TGF-β leads to alter plasticity of hypoxic cancer cells in tumor microenvironment. *Pharmacology & Therapeutics* **250,** 108519 (2023).
63. Suzuki, A., Maeda, T., Baba, Y., Shimamura, K. & Kato, Y. Acidic extracellular pH promotes epithelial mesenchymal transition in Lewis lung carcinoma model. *Cancer Cell International* **14,** 129 (2014).
64. Craene, B. D. & Berx, G. Regulatory networks defining EMT during cancer initiation and progression. *Nature Reviews Cancer* **13,** 97–110 (2013).
65. Barry, S. T., Gabrilovich, D. I., Sansom, O. J., Campbell, A. D. & Morton, J. P. Therapeutic targeting of tumour myeloid cells. *Nature Reviews Cancer* **23,** 216–237 (2023).
66. Colegio, O. R., Chu, N.-Q., Szabo, A. L., *et al.* Functional polarization of tumour-associated macrophages by tumour-derived lactic acid. *Nature* **513,** 559–563 (2014).
67. Selleri, S., Bifsha, P., Civini, S., *et al.* Human mesenchymal stromal cell-secreted lactate induces M2-macrophage differentiation by metabolic reprogramming. *Oncotarget* **7,** 30193–30210 (2016).
68. Bellocq, A., Suberville, S., Philippe, C., *et al.* Low Environmental pH Is Responsible for the Induction of Nitric-oxide Synthase in Macrophages. *Journal of Biological Chemistry* **273,** 5086–5092 (1998).
69. Husain, Z., Huang, Y., Seth, P. & Sukhatme, V. P. Tumor-Derived Lactate Modifies Antitumor Immune Response: Effect on Myeloid-Derived Suppressor Cells and NK Cells. *The Journal of Immunology* **191,** 1486–1495 (2013).

70. Cabeza-Cabrerizo, M., Cardoso, A., Minutti, C. M., Pereira Da Costa, M. & Reis E Sousa, C. Dendritic Cells Revisited. *Annual Review of Immunology* **39,** 131–166 (2021).

71. Ma, Y., Shurin, G. V., Peiyuan, Z. & Shurin, M. R. Dendritic Cells in the Cancer Microenvironment. *Journal of Cancer* **4,** 36–44 (2013).

72. Hargadon, K. M. Tumor-Altered Dendritic Cell Function: Implications for Anti-Tumor Immunity. *Frontiers in Immunology* **4** (2013).

73. Michea, P., Noël, F., Zakine, E., *et al.* Adjustment of dendritic cells to the breast-cancer microenvironment is subset specific. *Nature Immunology* **19,** 885–897 (2018).

74. Del Prete, A., Salvi, V., Soriani, A., *et al.* Dendritic cell subsets in cancer immunity and tumor antigen sensing. *Cellular & Molecular Immunology* **20,** 432–447 (2023).

75. Gottfried, E., Kunz-Schughart, L. A., Ebner, S., *et al.* Tumor-derived lactic acid modulates dendritic cell activation and antigen expression. *Blood* **107,** 2013–2021 (2006).

76. Nasi, A., Fekete, T., Krishnamurthy, A., *et al.* Dendritic Cell Reprogramming by Endogenously Produced Lactic Acid. *The Journal of Immunology* **191,** 3090–3099 (2013).

77. Li, X., Yuan, F.-L., Zhao, Q.-Y., *et al.* Acid-Sensing Ion Channels Contribute to the Effect of Acidosis on the Function of Dendritic Cells. *The Journal of Immunology* **186,** 6647–6647 (2011).

78. Heras-Murillo, I., Adán-Barrientos, I., Galán, M., Wculek, S. K. & Sancho, D. Dendritic cells as orchestrators of anticancer immunity and immunotherapy. *Nature Reviews Clinical Oncology* **21,** 257–277 (2024).

79. Sun, L., Su, Y., Jiao, A., Wang, X. & Zhang, B. T cells in health and disease. *Signal Transduction and Targeted Therapy* **8,** 235 (2023).

80. Fischer, K., Hoffmann, P., Voelkl, S., *et al.* Inhibitory effect of tumor cell–derived lactic acid on human T cells. *Blood* **109,** 3812–3819 (2007).

81. Chang, C.-H., Qiu, J., O'Sullivan, D., *et al.* Metabolic Competition in the Tumor Microenvironment Is a Driver of Cancer Progression. *Cell* **162,** 1229–1241 (2015).

82. Ho, P.-C., Bihuniak, J. D., Macintyre, A. N., *et al.* Phosphoenolpyruvate Is a Metabolic Checkpoint of Anti-tumor T Cell Responses. *Cell* **162,** 1217–1228 (2015).

83. Wolf, N. K., Kissiov, D. U. & Raulet, D. H. Roles of natural killer cells in immunity to cancer, and applications to immunotherapy. *Nature Reviews Immunology* **23,** 90–105 (2023).

84. Crane, C. A., Austgen, K., Haberthur, K., *et al.* Immune evasion mediated by tumor-derived lactate dehydrogenase induction of NKG2D ligands on myeloid cells in glioblastoma patients. *Proceedings of the National Academy of Sciences* **111,** 12823–12828 (2014).

85. Islam, A., Li, S. S., Oykhman, P., *et al.* An Acidic Microenvironment Increases NK Cell Killing of Cryptococcus neoformans and Cryptococcus gattii by Enhancing Perforin Degranulation. *PLoS Pathogens* **9** (ed Klein, B. S.) e1003439 (2013).

86. Hoffman, W., Lakkis, F. G. & Chalasani, G. B Cells, Antibodies, and More. *Clinical Journal of the American Society of Nephrology* **11,** 137–154 (2016).

87. Downs-Canner, S. M., Meier, J., Vincent, B. G. & Serody, J. S. B Cell Function in the Tumor Microenvironment. *Annual Review of Immunology* **40,** 169–193 (2022).

88. Watanabe, H., Matsumaru, H., Ooishi, A., *et al.* Optimizing pH Response of Affinity between Protein G and IgG Fc. *Journal of Biological Chemistry* **284,** 12373–12383 (2009).

89. Cairns, R., Papandreou, I. & Denko, N. Overcoming Physiologic Barriers to Cancer Treatment by Molecularly Targeting the Tumor Microenvironment. *Molecular Cancer Research* **4,** 61–70 (2006).

90. Thews, O., Gassner, B., Kelleher, D. K., Schwerd, G. & Gekle, M. Impact of Extracellular Acidity on the Activity of P-glycoprotein and the Cytotoxicity of Chemotherapeutic Drugs. *Neoplasia* **8,** 143–152 (2006).

91. Ward, C., Meehan, J., Gray, M. E., *et al.* The impact of tumour pH on cancer progression: strategies for clinical intervention. *Exploration of Targeted Anti-tumor Therapy* **1,** 71–100 (2020).

92. Cowan, D. S. & Tannock, I. F. Factors that influence the penetration of methotrexate through solid tissue. *International Journal of Cancer* **91,** 120–125 (2001).

93. Wassermann, K. & Bundgaard, H. Kinetics of the acid-catalyzed hydrolysis of doxorubicin. *International Journal of Pharmaceutics* **14,** 73–78 (1983).

94. Dewhirst, M. W., Cao, Y. & Moeller, B. Cycling hypoxia and free radicals regulate angiogenesis and radiotherapy response. *Nature Reviews Cancer* **8,** 425–437 (2008).

95. Aubert, L., Bastien, E., Renoult, O., *et al.* Tumor acidosis-induced DNA damage response and tetraploidy enhance sensitivity to ATM and ATR inhibitors. *EMBO Reports* **25,** 1469–1489 (2024).

96. Huang, R.-X. & Zhou, P.-K. DNA damage response signaling pathways and targets for radiotherapy sensitization in cancer. *Signal Transduction and Targeted Therapy* **5,** 60 (2020).

97. Park, H. J., Lyons, J. C., Ohtsubo, T. & Song, C. W. Acidic environment causes apoptosis by increasing caspase activity. *British Journal of Cancer* **80,** 1892–1897 (1999).

98. Sharma, V., Kaur, R., Bhatnagar, A. & Kaur, J. Low-pH-induced apoptosis: role of endoplasmic reticulum stress-induced calcium permeability and mitochondria-dependent signaling. *Cell Stress and Chaperones* **20,** 431–440 (2015).

99. Lee, H.-S., Park, H. J., Lyons, J. C., *et al.* Radiation-induced apoptosis in different pH environments in vitro. *International Journal of Radiation Oncology*Biology*Physics* **38,** 1079–1087 (1997).

100. Park, H. J., Lyons, J. C., Ohtsubo, T. & Song, C. W. Cell cycle progression and apoptosis after irradiation in an acidic environment. *Cell Death & Differentiation* **7,** 729–738 (2000).

101. Park, H., Lyons, J. C., Griffin, R. J., Lim, B. U. & Song, C. W. Apoptosis and Cell Cycle Progression in an Acidic Environment after Irradiation. *Radiation Research* **153,** 295–304 (2000).

102. Pilon-Thomas, S., Kodumudi, K. N., El-Kenawi, A. E., *et al.* Neutralization of Tumor Acidity Improves Antitumor Responses to Immunotherapy. *Cancer Research* **76,** 1381–1390 (2016).

103. Robey, I. F., Baggett, B. K., Kirkpatrick, N. D., *et al.* Bicarbonate Increases Tumor pH and Inhibits Spontaneous Metastases. *Cancer Research* **69,** 2260–2268 (2009).

104. Calcinotto, A., Filipazzi, P., Grioni, M., *et al.* Modulation of Microenvironment Acidity Reverses Anergy in Human and Murine Tumor-Infiltrating T Lymphocytes. *Cancer Research* **72,** 2746–2756 (2012).

105. Subbarao, N. K. & Parente, R. A. pH-Dependent Bilayer Destabilization by an Amphipathic Peptide. *Biochemistry* **26(11),** 2964–72.

106. Sakurai, Y., Hatakeyama, H., Sato, Y., *et al.* Endosomal escape and the knockdown efficiency of liposomal-siRNA by the fusogenic peptide shGALA. *Biomaterials* **32,** 5733–5742 (2011).

107. Miura, N., Shaheen, S. M., Akita, H., Nakamura, T. & Harashima, H. A KALA-modified lipid nanoparticle containing CpG-free plasmid DNA as a potential DNA vaccine carrier for antigen presentation and as an immune-stimulative adjuvant. *Nucleic Acids Research* **43,** 1317–1331 (2015).

108. Bhattacharya, S., Prajapati, B. G. & Singh, S. A critical review on the dissemination of PH and stimuli-responsive polymeric nanoparticular systems to improve drug delivery in cancer therapy. *Critical Reviews in Oncology/Hematology* **185,** 103961 (2023).

109. He, X., Li, J., An, S. & Jiang, C. pH-sensitive drug-delivery Systems for Tumor Targeting. *Therapeutic Delivery* **4,** 1499–1510 (2013).

110. Kanamala, M., Wilson, W. R., Yang, M., Palmer, B. D. & Wu, Z. Mechanisms and biomaterials in pH-responsive tumour targeted drug delivery: A review. *Biomaterials* **85,** 152–167 (2016).

111. Liu, S., Luo, X., Liu, S., *et al.* Acetazolamide-Loaded pH-Responsive Nanoparticles Alleviating Tumor Acidosis to Enhance Chemotherapy Effects. *Macromolecular Bioscience* **19,** 1800366 (2019).

112. Liao, S., Wu, G., Xie, Z., *et al.* pH regulators and their inhibitors in tumor microenvironment. *European Journal of Medicinal Chemistry* **267,** 116170 (2024).

113. Cappellesso, F., Orban, M.-P., Shirgaonkar, N., *et al.* Targeting the bicarbonate transporter SLC4A4 overcomes immunosuppression and immunotherapy resistance in pancreatic cancer. *Nature Cancer* **3,** 1464–1483 (2022).

114. Zheng, G. X. Y., Terry, J. M., Belgrader, P., *et al.* Massively parallel digital transcriptional profiling of single cells. *Nature Communications* **8,** 14049 (2017).

115. Lun, A. T. L., Riesenfeld, S., Andrews, T., *et al.* EmptyDrops: distinguishing cells from empty droplets in droplet-based single-cell RNA sequencing data. *Genome Biology* **20,** 63 (2019).

116. Huang, X. & Huang, Y. Cellsnp-lite: an efficient tool for genotyping single cells. *Bioinformatics* **37** (ed Alkan, C.) 4569–4571 (2021).

117. Huang, Y., McCarthy, D. J. & Stegle, O. Vireo: Bayesian demultiplexing of pooled single-cell RNA-seq data without genotype reference. *Genome Biology* **20,** 273 (2019).

118. Germain, P.-L., Lun, A., Meixide, C. G., Macnair, W. & Robinson, M. D. Doublet identification in single-cell sequencing data. *F1000 Research* **10** (2022).

119. Wolock, S. L., Lopez, R. & Klein, A. M. Scrublet: Computational Identification of Cell Doublets in Single-Cell Transcriptomic Data. *Cell Systems* **8,** 281–291.e9 (2019).

120. McGinnis, C. S., Murrow, L. M. & Gartner, Z. J. DoubletFinder: Doublet Detection in Single-Cell RNA Sequencing Data Using Artificial Nearest Neighbors. *Cell Systems* **8,** 329–337.e4 (2019).

121. Young, M. D. & Behjati, S. SoupX removes ambient RNA contamination from droplet-based single-cell RNA sequencing data. *GigaScience* **9,** giaa151 (2020).

122. Hao, Y., Hao, S., Andersen-Nissen, E., *et al.* Integrated analysis of multimodal single-cell data. *Cell* **184,** 3573–3587.e29 (2021).

123. Ahern, D. J., Ai, Z., Ainsworth, M., *et al.* A blood atlas of COVID-19 defines hallmarks of disease severity and specificity. *Cell* **185,** 916–938.e58 (2022).

124. Burel, J. G., Pomaznoy, M., Lindestam Arlehamn, C. S., *et al.* Circulating T cell-monocyte complexes are markers of immune perturbations. *eLife* **8,** e46045 (2019).

125. Zheng, L., Qin, S., Si, W., *et al.* Pan-cancer single-cell landscape of tumor-infiltrating T cells. *Science* **374,** abe6474 (2021).

126. Morabito, S., Reese, F., Rahimzadeh, N., Miyoshi, E. & Swarup, V. hdWGCNA identifies co-expression networks in high-dimensional transcriptomics data. *Cell Reports Methods* **3,** 100498 (2023).

127. Aibar, S., González-Blas, C. B., Moerman, T., *et al.* SCENIC: single-cell regulatory network inference and clustering. *Nature Methods* **14,** 1083–1086 (2017).

128. Polasky, C., Wendt, F., Pries, R. & Wollenberg, B. Platelet Induced Functional Alteration of CD4+ and CD8+ T Cells in HNSCC. *International Journal of Molecular Sciences* **21,** 7507 (2020).

129. Green, S. A., Smith, M., Hasley, R. B., *et al.* Activated platelet–T-cell conjugates in peripheral blood of patients with HIV infection: coupling coagulation/inflammation and T cells. *AIDS* **29,** 1297–1308 (2015).

130. Khavkin, T., Kuchler, M., Carl, M., *et al.* Activation and enhanced contact of human T-lymphocytes with autologous red blood cells are required for their stable adherence at 37°. *Virchows Archiv B Cell Pathology Including Molecular Pathology* **64,** 351–359 (1993).

131. Pellin, D., Loperfido, M., Baricordi, C., *et al.* A comprehensive single cell transcriptional landscape of human hematopoietic progenitors. *Nature Communications* **10,** 2395 (2019).

132. Luecken, M. D., Büttner, M., Chaichoompu, K., *et al.* Benchmarking atlas-level data integration in single-cell genomics. *Nature Methods* **19,** 41–50 (2022).

133. Korsunsky, I., Millard, N., Fan, J., *et al.* Fast, sensitive and accurate integration of single-cell data with Harmony. *Nature Methods* **16,** 1289–1296 (2019).

134. Argelaguet, R., Cuomo, A. S. E., Stegle, O. & Marioni, J. C. Computational principles and challenges in single-cell data integration. *Nature Biotechnology* **39,** 1202–1215 (2021).

135. Fu, D., Li, J., Wei, J., *et al.* HMGB2 is associated with malignancy and regulates Warburg effect by targeting LDHB and FBP1 in breast cancer. *Cell Communication and Signaling* **16,** 8 (2018).

136. Han, W., Zhou, H., Zhang, X., *et al.* HMGB2 is a biomarker associated with poor prognosis promoting radioresistance in glioma by targeting base excision repair pathway. *Translational Oncology* **45,** 101977 (2024).

137. Neubert, E. N., DeRogatis, J. M., Lewis, S. A., *et al.* HMGB2 regulates the differentiation and stemness of exhausted CD8+ T cells during chronic viral infection and cancer. *Nature Communications* **14,** 5631 (2023).

138. Zhang, L., Zhao, Y., Yang, J., *et al.* CTSL, a prognostic marker of breast cancer, that promotes proliferation, migration, and invasion in cells in triple-negative breast cancer. *Frontiers in Oncology* **13,** 1158087 (2023).

139. Sudhan, D. R. & Siemann, D. W. Cathepsin L targeting in cancer treatment. *Pharmacology & Therapeutics* **155,** 105–116 (2015).

140. Yu, K., Kuang, L., Fu, T., *et al.* CREM Is Correlated With Immune-Suppressive Microenvironment and Predicts Poor Prognosis in Gastric Adenocarcinoma. *Frontiers in Cell and Developmental Biology* **9,** 697748 (2021).

141. Kerdiles, Y. M., Stone, E. L., Beisner, D. L., *et al.* Foxo Transcription Factors Control Regulatory T Cell Development and Function. *Immunity* **33,** 890–904 (2010).

142. Ouyang, W., Beckett, O., Ma, Q., *et al.* Foxo proteins cooperatively control the differentiation of Foxp3+ regulatory T cells. *Nature Immunology* **11,** 618–627 (2010).

143. Thompson, M. G., Larson, M., Vidrine, A., *et al.* FOXO3–NF-$\varkappa$B RelA Protein Complexes Reduce Proinflammatory Cell Signaling and Function. *The Journal of Immunology* **195,** 5637–5647 (2015).

144. Baumann, S., Hess, J., Eichhorst, S. T., *et al.* An unexpected role for FosB in activation-induced cell death of T cells. *Oncogene* **22,** 1333–1339 (2003).

145. Squair, J. W., Gautier, M., Kathe, C., *et al.* Confronting false discoveries in single-cell differential expression. *Nature Communications* **12,** 5692 (2021).

146. Zimmerman, K. D., Espeland, M. A. & Langefeld, C. D. A practical solution to pseudoreplication bias in single-cell studies. *Nature Communications* **12,** 738 (2021).

147. Morris, M. E. & Felmlee, M. A. Overview of the Proton-coupled MCT (SLC16A) Family of Transporters: Characterization, Function and Role in the Transport of the Drug of Abuse γ-Hydroxybutyric Acid. *The AAPS Journal* **10,** 311 (2008).

148. Zhou, B., Lin, W., Long, Y., *et al.* Notch signaling pathway: architecture, disease, and therapeutics. *Signal Transduction and Targeted Therapy* **7,** 95 (2022).

149. Petrik, J., Lauks, S., Garlisi, B. & Lawler, J. Thrombospondins in the tumor microenvironment. *Seminars in Cell & Developmental Biology* **155,** 3–11 (2024).

150. Omatsu, M., Nakanishi, Y., Iwane, K., *et al.* THBS1-producing tumor-infiltrating monocyte-like cells contribute to immunosuppression and metastasis in colorectal cancer. *Nature Communications* **14,** 5534 (2023).

151. Daubon, T., Léon, C., Clarke, K., *et al.* Deciphering the complex role of thrombospondin-1 in glioblastoma development. *Nature Communications* **10,** 1146 (2019).

152. Das, S., Rai, A. & Rai, S. N. Differential Expression Analysis of Single-Cell RNA-Seq Data: Current Statistical Approaches and Outstanding Challenges. *Entropy* **24,** 995 (2022).

153. Pittet, M. J., Michielin, O. & Migliorini, D. Clinical relevance of tumour-associated macrophages. *Nature Reviews Clinical Oncology* **19,** 402–421 (2022).

154. Zyla, J., Marczyk, M., Weiner, J. & Polanska, J. Ranking metrics in gene set enrichment analysis: do they matter? *BMC Bioinformatics* **18,** 256 (2017).

155. Guo, Q., Jin, Y., Chen, X., *et al.* NF-$\varkappa$B in biology and targeted therapy: new insights and translational implications. *Signal Transduction and Targeted Therapy* **9,** 53 (2024).

156. Yu, H., Lin, L., Zhang, Z., Zhang, H. & Hu, H. Targeting NF-$\varkappa$B pathway for the therapy of diseases: mechanism and clinical study. *Signal Transduction and Targeted Therapy* **5,** 209 (2020).

157. Li, J., Dong, T., Wu, Z., Zhu, D. & Gu, H. The effects of MYC on tumor immunity and immunotherapy. *Cell Death Discovery* **9,** 103 (2023).

158. Rohban, S. & Campaner, S. Myc induced replicative stress response: How to cope with it and exploit it. *Biochimica et Biophysica Acta (BBA) - Gene Regulatory Mechanisms* **1849,** 517–524 (2015).

159. Li, X., Xiang, Y., Li, F., *et al.* WNT/β-Catenin Signaling Pathway Regulating T Cell-Inflammation in the Tumor Microenvironment. *Frontiers in Immunology* **10,** 2293 (2019).

160. Quandt, J., Arnovitz, S., Haghi, L., *et al.* Wnt–β-catenin activation epigenetically reprograms Treg cells in inflammatory bowel disease and dysplastic progression. *Nature Immunology* **22,** 471–484 (2021).

161. Nie, Z., Chen, M., Wen, X., *et al.* Endoplasmic Reticulum Stress and Tumor Microenvironment in Bladder Cancer: The Missing Link. *Frontiers in Cell and Developmental Biology* **9,** 683940 (2021).

162. Sun, S., Han, J., Jr, W. M. R., *et al.* Endoplasmic reticulum stress as a correlate of cytotoxicity in human tumor cells exposed to diindolylmethane in vitro. *Cell Stress* **9,** 76–87 (2004).

163. Zhang, W., Shi, Y., Oyang, L., *et al.* Endoplasmic reticulum stress—a key guardian in cancer. *Cell Death Discovery* **10,** 343 (2024).

164. Tan, Y., Wang, M., Zhang, Y., *et al.* Tumor-Associated Macrophages: A Potential Target for Cancer Therapy. *Frontiers in Oncology* **11,** 693517 (2021).

165. Liu, Z.-L., Chen, H.-H., Zheng, L.-L., Sun, L.-P. & Shi, L. Angiogenic signaling pathways and anti-angiogenic therapy for cancer. *Signal Transduction and Targeted Therapy* **8,** 198 (2023).

166. Johnstone, S. E. & Baylin, S. B. Stress and the epigenetic landscape: a link to the pathobiology of human diseases? *Nature Reviews Genetics* **11,** 806–812 (2010).

167. Soriano-Baguet, L. & Brenner, D. Metabolism and epigenetics at the heart of T cell function. *Trends in Immunology* **44,** 231–244 (2023).

168. Hathaway-Schrader, J. D. & Novince, C. M. GPR65, a novel regulator of helper T-cell polarization in inflammatory bowel disease. *Clinical and Translational Medicine* **12,** e857 (2022).

169. Fan, J., Liu, J., Zhang, B., *et al.* GPR65 contributes to constructing immunosuppressive microenvironment in glioma. *Neurosurgical Review* **47,** 417 (2024).

170. Wang, L., Sun, L., Sun, H., *et al.* GPR65 as a potential immune checkpoint regulates the immune microenvironment according to pan-cancer analysis. *Heliyon* **9,** e13617 (2023).

171. Qi, J., Liu, S. & Zhang, Z. What role does GPR65 play in the progression of osteosarcoma? Its mechanism and clinical significance. *Cancer Cell International* **24,** 31 (2024).

172. Hosseinpour, M., Khamechian, T. & Shahrokh, S. Peritoneal Potassium and pH Measurement in Early Diagnosis of Acute Mesenteric Ischemia in Rats. *Archives of Trauma Research* **3** (2014).

173. Punnia-Moorthy, A. Evaluation of pH changes in inflammation of the subcutaneous air pouch lining in the rat, induced by carrageenan, dextran and staphylococcus aureus. *Journal of Oral Pathology & Medicine* **16,** 36–44 (1987).

174. Stoeckius, M., Hafemeister, C., Stephenson, W., *et al.* Simultaneous epitope and transcriptome measurement in single cells. *Nature Methods* **14,** 865–868 (2017).

175. Dvorak, H. F. Tumors: Wounds That Do Not Heal—Redux. *Cancer Immunology Research* **3,** 1–11 (2015).

176. Danecek, P., Bonfield, J. K., Liddle, J., *et al.* Twelve years of SAMtools and BCFtools. *GigaScience* **10,** giab008 (2021).

177. Ritchie, M. E., Phipson, B., Wu, D., *et al.* limma powers differential expression analyses for RNA-sequencing and microarray studies. *Nucleic Acids Research* **43,** e47–e47 (2015).

178. Chang, C. C., Chow, C. C., Tellier, L. C., *et al.* Second-generation PLINK: rising to the challenge of larger and richer datasets. *GigaScience* **4,** 7 (2015).

179. R Core Team. R: A Language and Environment for Statistical Computing (2021).

180. Aran, D., Looney, A. P., Liu, L., *et al.* Reference-based analysis of lung single-cell sequencing reveals a transitional profibrotic macrophage. *Nature Immunology* **20,** 163–172 (2019).

181. Danecek, P., Auton, A., Abecasis, G., *et al.* The variant call format and VCFtools. *Bioinformatics* **27,** 2156–2158 (2011).

182. Fang, H., Knezevic, B., Burnham, K. L. & Knight, J. C. XGR software for enhanced interpretation of genomic summary data, illustrated by application to immunological traits. *Genome Medicine* **8,** 129 (2016).